Interaction of the neuronal multipurpose X11a protein with the copper chaperone CCS

Duquesne, A.E.

Citation

Duquesne, A. E. (2005, October 17). *Interaction of the neuronal multipurpose X11a protein with the copper chaperone CCS*. Retrieved from https://hdl.handle.net/1887/3486

Interaction of the neuronal multipurpose X11α protein with the copper chaperone CCS

PROEFSCHRIFT

ter verkrijging van de graad van Doctor and de Universiteit Leiden,
op gezag van de Rector Magnificus Dr D.D. Breimer,
hoogleraar in de faculteit der Wiskunde en
Natuurwetenschappen en die der Geneeskunde,
volgens besluit van het College voor Promoties te verdedigen op
maandag 17 oktober 2005
te klokke 16.15 uur

door

Aude Elodie Duquesne

geboren te Coulommiers in 1977

Promotiecommissie

Promotor: Prof. Dr. G.W. Canters

Co-promotor: Dr. M. Ubbink

Referent: Prof. Dr. C.W.A. Pleij

Overigen leden: Prof. Dr. J. Brouwer

                   Dr. G.W. Vuister (Radboud Universiteit Nijmegen)

A mon arrière-grand-père, Emile Filiatreaud

A mes grands-parents, Mimie et Gaston Corbin

Table of content

Chapter I

General introduction

PREFACE

Proteins, nucleic acids and polysaccharides are the macromolecules of life. Throughout the birth, growth and death of the cell, these macromolecules interact with each other to ensure propagation of messages not only within the cell but also between cells. For instance, proteins, which represent about 15% of a cell in mass, are the workhorses of the cell. Protein-protein interactions are involved at each and every step of cellular events, such as DNA/RNA synthesis and degradation, protein synthesis, folding and degradation, signal transduction (within the cell and between cells), regulation of protein activity, and immune response.

Therefore, understanding protein-protein interactions is essential to understand the processes that occur in the cell, and ultimately to develop cures for the deficient processes.

The PhD research presented here aims at characterizing the molecular details of the interaction between a protein involved in copper homeostasis (CCS[1]) and the neuronal adaptor X11α, originally discovered by McLoughlin *et al.* (McLoughlin *et al.*, 2001).

Some background information about copper homeostasis and the role of chaperones will first be provided. Next, general features of X11 proteins domains will be discussed. Finally, the work presented in this thesis will be outlined.

---

[1] CCS: <u>c</u>opper <u>c</u>haperone for <u>s</u>uperoxide dismutase 1 (see pg. 117 for a complete list of abbreviations)
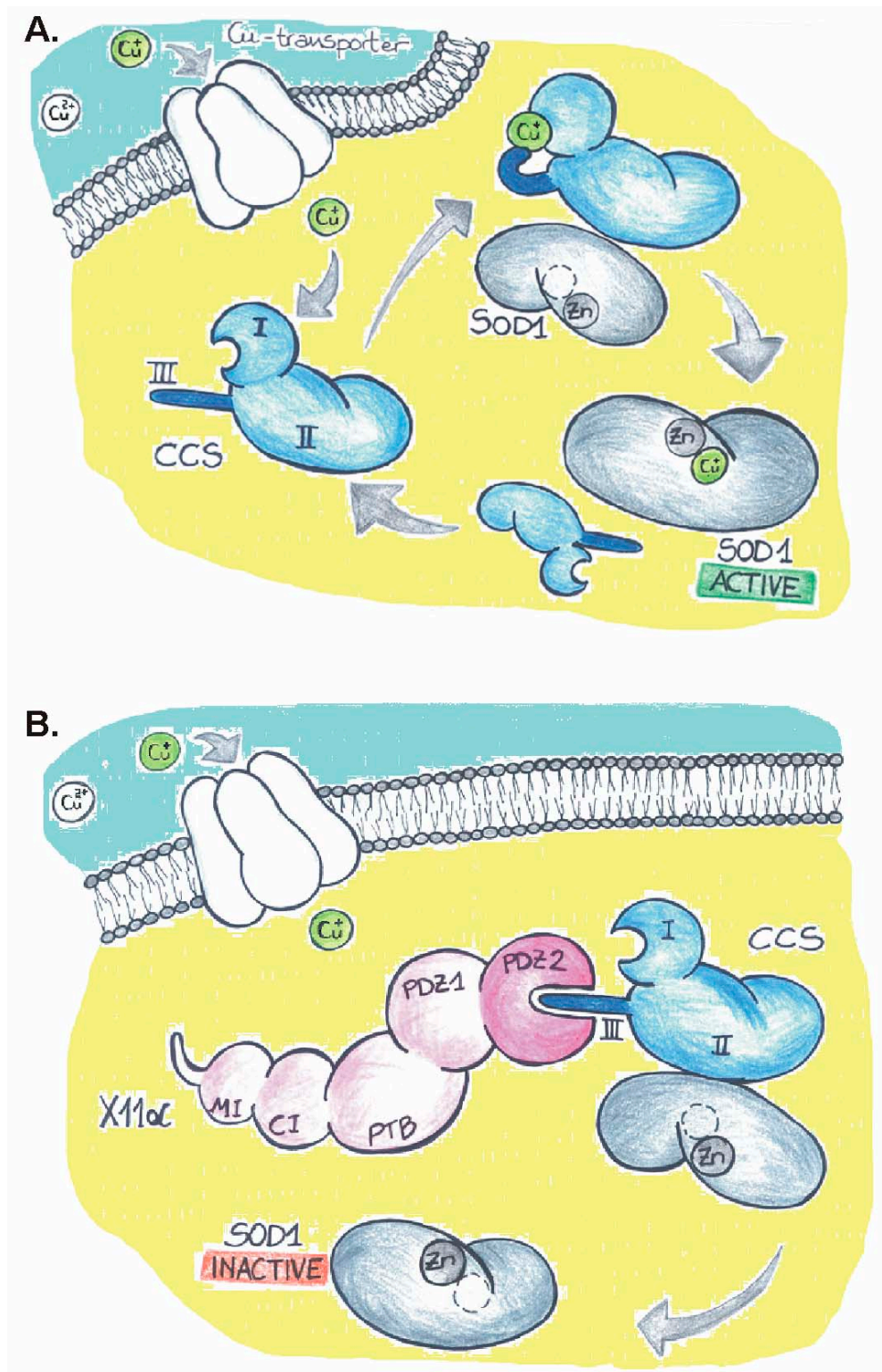
Figure 1.1: **A.** Schematic representation of the role of CCS. The extracellular divalent copper (white circle Cu²⁺) is reduced to Cu⁺ (green circle) and then enters the cell via a membrane-bound copper transporter (in white). Inside the cell, the copper is taken up by CCS, which delivers it to the target, resulting in an active SOD1. **B.** Schematic representation of the situation in the presence of the neuron protein X11α. CCSIII (in dark blue) binds the PDZ2 domain of X11α (in dark pink) and transfer of copper to SOD1 can no longer occur, resulting in an inactive SOD1.

I.1 - COPPER HOMEOSTASIS

Metals are involved in many essential biological reactions. Necessary as they are, they are also potentially toxic for cells and must therefore be carefully handled.

In the last decade it has been discovered that cells are equipped with an elaborate system of transport for copper, so that free copper ions are virtually absent inside the cell (Rae *et al.*, 1999). For instance, *Saccharomyces cerevisiae* possesses repeated DNA sequences (named CuREs) at the promoter region of the genes coding for the membrane copper transporters Ctr1, Ctr3 and Fre1. These repeats are the target of a nuclear sensor protein specific for copper ions (Mac1) that detects the amount of copper available (Labbe *et al.*, 1997). At low copper concentration, Mac1 binds the CuREs and the expression of the transporters is activated (YamaguchiIwai *et al.*, 1997; Jensen *et al.*, 1998; Martins *et al.*, 1998; Joshi *et al.*, 1999). Under higher copper level, Mac1 undergoes conformational changes so that it is released from the CuREs and the production of the membrane transporters is terminated (Labbe *et al.*, 1997).

Divalent copper, Cu(II), present outside the cell is reduced to Cu(I) by iron-containing membrane proteins Fre1 and Fre2 (Dancis, 1998; Martins *et al.*, 1998), illustrating in addition a tight coupling between copper and iron homeostasis. Cu(I) is allowed then to cross the membrane by the action of high-affinity transporters(see Figure 1.1), Ctr1 and Ctr3 (Dancis *et al.*, 1994; Knight *et al.*, 1996; Pena *et al.*, 2000). Once inside the cell, metallochaperones shuttle the copper ions to their target proteins. There exists a specific chaperone for each target, and each compartment within the cell possesses its own chaperone-target system. The chaperone Cox17 brings copper to the mitochondrial cytochrome c oxidase (Glerum *et al.*, 1996) involved in respiration. Atx1 carries it to the high-affinity iron transporter Fet3 via the membrane bound Ccc2 protein at the Golgi apparatus (Lin *et al.*, 1997; Pufahl *et al.*, 1997), and CCS shuttles copper to the SOD1 (**s**uper**o**xide **d**ismutase 1) (Culotta *et al.*, 1997), an enzyme involved in removal of **r**eactive **o**xygen **s**pecies (ROS) (Harrison *et al.*, 1999; Pena *et al.*, 1999; O'Halloran and Culotta, 2000).

This system of Cu transport is conserved across many life forms, as homologues of the above mentioned yeast chaperones have been identified in bacteria, plants,

worms and mammals (Culotta *et al.*, 1997; Klomp *et al.*, 1997; Himelblau *et al.*, 1998; Nishihara *et al.*, 1998; Wakabayashi *et al.*, 1998; Hiromura and Sakurai, 1999; Lockhart and Mercer, 2000; Hiromura *et al.*, 2000; Wong *et al.*, 2000; Solioz *et al.*, 2003; Silahtaroglu *et al.*, 2004).

Impairment in the physiological function of one of the proteins involved in copper transport, or in the target protein has been related to neurodegenerative disorders. For example, amyotrophic lateral sclerosis (ALS) is caused by mutations resulting in an inactive SOD1 (Goto *et al.*, 2000). Menkes and Wilson's diseases are associated with copper shortage and excess, respectively, due to malfunctioning of Ccc2 homologues (Waggoner *et al.*, 1999).

I.2 - THE COPPER CHAPERONE FOR SUPEROXIDE DISMUTASE 1

Three domains have been identified in CCS (Lamb *et al.*, 1999; Rosenzweig *et al.*, 1999) as depicted in Figure 1.1. The N-terminal domain (CCSI) exhibits high homology with ATX1 (mentioned above), and hence was named ATX1-like domain. It is supposed to bind Cu(I). The central domain (CCSII) resembles the target SOD1, hence the name SOD1-like domain; it is believed to be involved in target recognition. Finally, the C-terminal domain of the human CCS (CCSIII) consists of 40 residues and contains a Cys–X–Cys motif, suggested to bind Cu(I) (Falconi *et al.*, 1999; Rosenzweig and O'Halloran, 2000).

As mentioned above, CCS is essential for SOD1 activation (Culotta *et al.*, 1997). Surprisingly, it has been shown that CCSII and CCSIII, but not CCSI, are necessary for copper loading into SOD1 *in vivo*. CCSI is required only under copper starvation conditions (Schmidt *et al.*, 1999; Schmidt *et al.*, 2000).

The role of CCSIII remained unclear until crystal structures of the yeast homologue of CCS were solved. Comparative studies of the structure of the native CCS alone and in complex with SOD1 (Lamb *et al.*, 1999; Lamb *et al.*, 2001) provided some clues about the mechanism of copper delivery between CCS and SOD1. Those structures

revealed that the SOD1-like domain of CCS binds the target, and that CCSIII adopts a well-defined conformation in the complex with its two cysteines positioned close to the copper binding site of SOD1, while it was disordered and not observed in the structure of the native CCS. Furthermore, the structures show that the copper binding domain (ATX1-like) of CCS is too far from the target site of SOD1 for direct interaction. It was therefore suggested (Falconi *et al.*, 1999; Rosenzweig and O'Halloran, 2000) that the flexible CCSIII serves as a shuttle between the copper binding site of the ATX1-like domain of CCS and that of SOD1.

Also, a new partner of CCS was discovered in brain cells. McLoughlin *et al.* demonstrated that the human CCS and X11α, a neuronal protein related to Alzheimer's disease, interact via their third domain (CCSIII) and second PDZ[2] domain (PDZ2α), respectively (McLoughlin *et al.*, 2001). Consequently, SOD1 cannot acquire copper, and it fails to fulfill its essential physiological role (see Figure 1.1).

I.3 - THE NEURONAL ADAPTOR FAMILY X11

I.3.1 - General aspects

X11 proteins, also known as Mint proteins (for **M**unc18 **int**eracting protein), are so-called adaptor proteins. They contain multiple domains (see Figure 1.2) able to recruit proteins, resulting in the formation of large protein complexes as shown in Figure 1.3. The X11 family counts three members: α, β and γ (Swiss-Prot accession number Q02410, Q99767 and O96018, respectively). X11α and β are expressed only in the brain, while X11γ is expressed ubiquitously (Okamoto and Sudhof, 1997; Okamoto and Sudhof, 1998).

---

[2] PDZ: **p**ost-synaptic density-95 protein, **D**rosophila disks-large protein A, **z**ona occludens protein 1
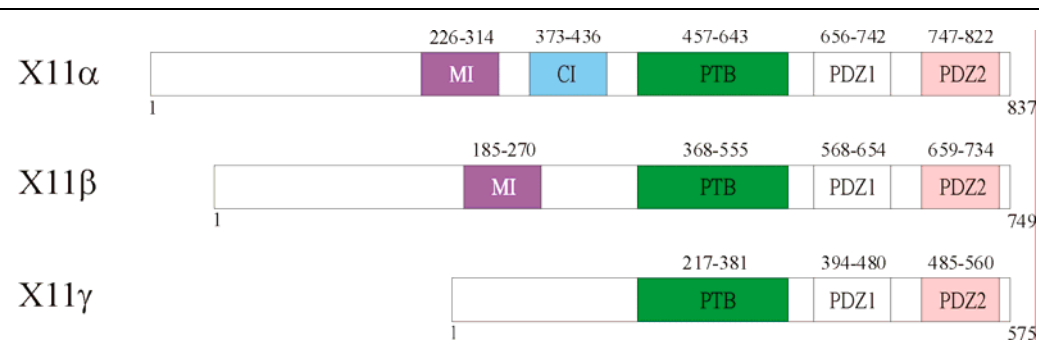
Figure 1.2: Schematic representation of the organization of the three X11 family members

All three contain a PTB (_p_hospho_t_yrosine _b_inding domain) and two PDZ domains, the role of which is explained below. The main differences are observed in the N-terminal domains: X11γ lacks the MI domain (_M_unc18a _i_nteracting _d_omain) present in the other two homologues. The function(s) of X11 protein(s) is(are) still a matter of debate and varies depending on the organism of study (Biederer _et al._, 2002).

The cartoons of Figure 1.3 show the organization and the various partners of all three X11 proteins known to date.
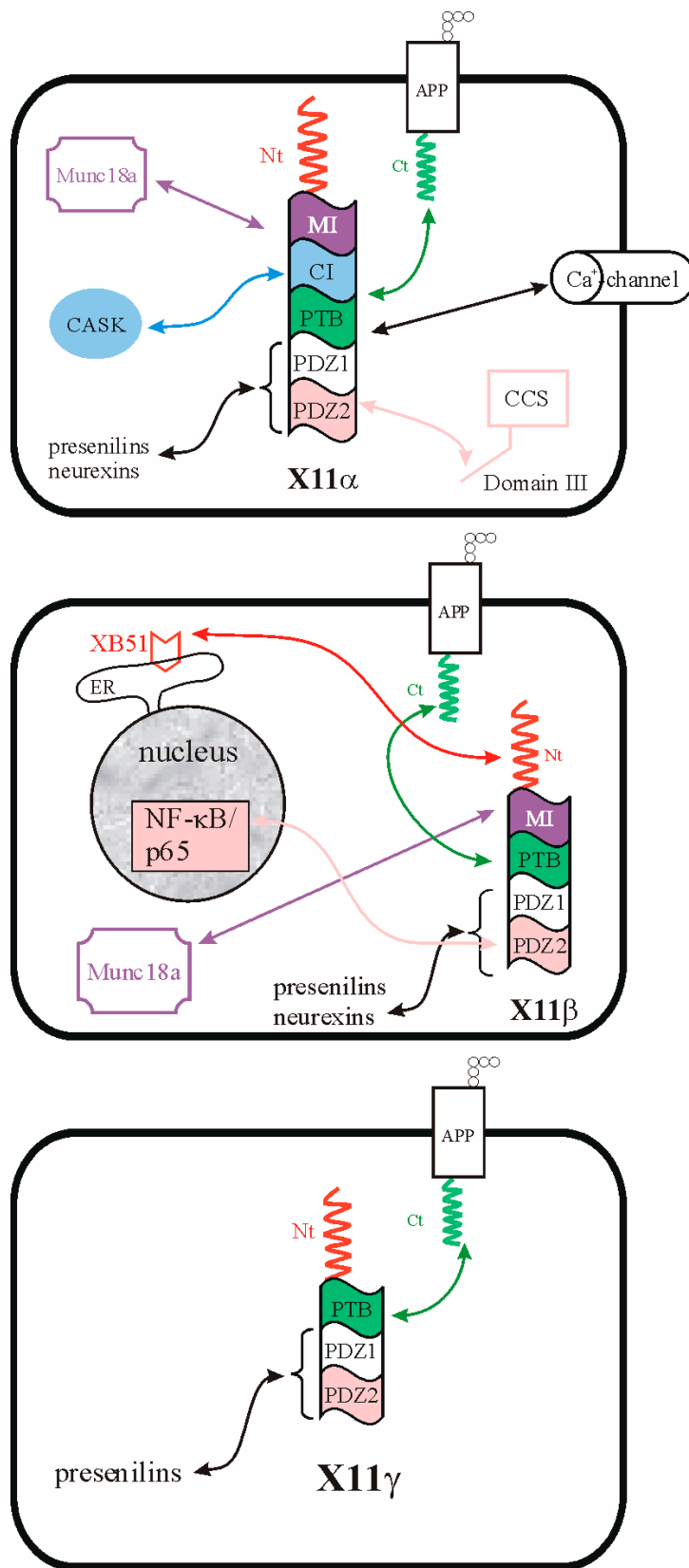
Figure 1.3: Scheme of the various partners of the three X11 family members (α, β and γ). See text for further explanations

I.3.2 - The PTB domain

The PTB domain is present in all three X11s. It binds the C-terminal domain of the amyloid precursor protein (APP) (Biederer *et al.*, 2002; Ho *et al.*, 2002) with the protection of cellular APP against degradation as a result, and a reduction of the production and the secretion of Aβ (the major component of the senile plaques and fibrils present in the brains of Alzheimer patients).

I.3.3 - The N-terminal domains (Nt)

X11α and β interact with Munc18a via their MI moiety (Okamoto and Sudhof, 1997; Ho *et al.*, 2002). Co-expression of Munc18a and any of the three X11s modulates the protective role of X11s against APP degradation. The presence of Munc18a suppresses the secretion of Aβ40 (one degradation product of APP) even more than in the presence of X11 alone. Surprisingly, the protective effect of X11γ on APP is also enhanced by the presence of Munc18a, although X11γ (which lacks the MI domain) is not able to interact directly with Munc18a.

X11α can also form a complex with CASK (another adaptor protein) via its unique CI domain. Simultaneously, CASK binds Veli (yet another family of adaptors). The formation of this trimer is believed to be the starting point of protein assembly at the synaptic junction for exocytosis and neurotransmission (Butz *et al.*, 1998).

The N-terminal part (Nt) of X11β has been shown to bind a protein located on the endoplasmic reticulum (XB51), inhibiting the above-mentioned Aβ40 secretion suppressor role of X11β (Lee *et al.*, 2000).

I.3.4 - The conserved PDZ domains

The functions of the two PDZ domains of X11s are still unclear. They seem to possess an unusual number of partners (as compared to other PDZ domains).

All three X11s have been shown to bind presenilins (the only protein known to date to be responsible for inherited Alzheimer) via either or both PDZ domains (Biederer *et al.*, 2002). The authors suggest that the enzymatic activity of presenilins (involved

in the degradation of APP) be inhibited when presenilins are in complex with X11s and APP together (and maybe more proteins).

X11α/β have been shown to bind neurexins (involved in neuronal exocytosis) via their PDZ domains (although it is not clear which one) (Biederer and Sudhof, 2000). The purpose of this interaction is thought to bring Munc18a at the synaptic membrane, where it is required for signal transmission.

The most N-terminal PDZ domain of X11α has been shown to interact with the carboxy-terminus of the presynaptic Ca^{2+} voltage-gated channel (Maximov *et al.*, 1999). The authors suggest that this interaction occurs in the presence of the above-mentioned trimer X11/CASK/Veli for neurotransmission.

In addition to its suppressing role of Aβ40 secretion mentioned earlier, X11β has been suggested to regulate the production of Aβ42 (another degradation product of APP) at the endoplasmic reticulum (Tomita *et al.*, 2000). Indeed, they have demonstrated that the second PDZ domain of X11β binds the transcription factor NF-κB/p65, repressing the expression of enzymes responsible for APP cleavage into Aβ42.

Furthermore, the C-terminal PDZ domain of X11α (as mentioned above) has been reported to interact with the third domain of CCS (McLoughlin *et al.*, 2001), suggesting a new role for X11α and PDZ domains.

I.4 - PDZ DOMAINS

I.4.1 - Roles

PDZ domains are present in a large number of proteins, often involved in signal transduction. Their role is to help the formation of protein complexes, usually at the plasma membrane, but also in the nucleus (for reviews see (Fanning and Anderson, 1999; Jelen *et al.*, 2003; van Ham and Hendriks, 2003). Despite a low sequence similarity among the PDZ domains, their structures are remarkably conserved, consisting of six β-strands and two α-helices (see Figure 1.4).
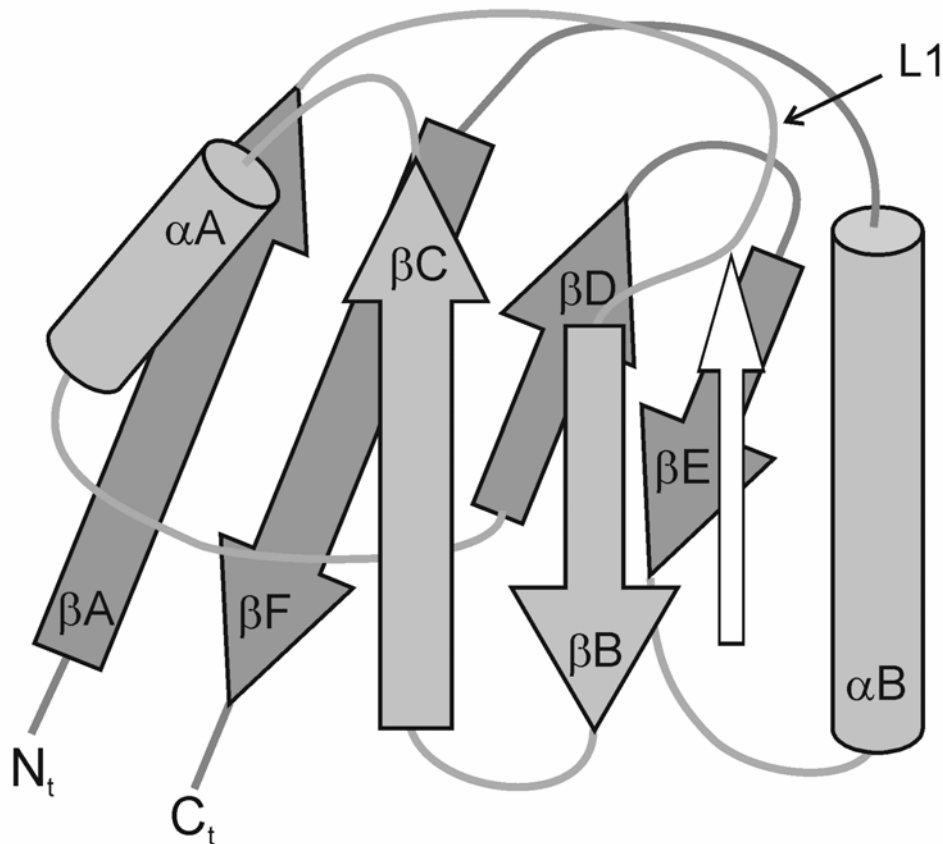
Figure 1.4: General fold of PDZ domains. The β-strands are annotated βA to βF; the α-helices are annotated αA and αB. The white arrow represents the canonical ligand with the carboxy-terminal group at the tip of the arrow.

I.4.2 - Modes of interaction and classification

The classical binding of the carboxy-terminal tail of partner proteins to PDZ domains occurs in a binding pocket located between βB and αB, creating an extension of the existing β sheet (see Figure 1.4). This interaction site consists of conserved residues situated in the L1 loop and the βB strand. It contains a conserved sequence motif (G/Q–L–G–F/I) on the PDZ domain and a conserved arginine N-terminal of this motif that is involved in coordination of the carboxy-terminus of the target via a water molecule. The interacting peptides have traditionally been grouped into four classes on the basis of their C-terminal sequences: Class I contains S/TxΦ* sequences (where Φ corresponds to any hydrophobic residue and * to the

carboxy terminus), Class II contains ΦxΦ*, Class III E/DxΦ* and Class IV VxD/E* sequences (Vaccaro and Dente, 2002). It is now well documented that PDZ domains are promiscuous, able to bind C-termini across classes (Palmer *et al.*, 2002; Walma *et al.*, 2002). PDZ domains are also capable of recognizing internal peptide motifs through the same binding groove (Hillier *et al.*, 1999), such as displayed by the interaction between the second PDZ domain of α1-syntrophin and the C-terminal β-finger of <u>n</u>itrous <u>o</u>xide <u>s</u>ynthase (NOS). Furthermore, PDZ domains have other interaction surfaces (Feng *et al.*, 2002; Feng *et al.*, 2003; Im *et al.*, 2003), and not only proteins but also phospholipids may serve as binding targets (Zimmermann *et al.*, 2002).

As a response to the increase in the variety of partners, new classifications of PDZ are regularly published. Bezprozvanny and Maximov (Bezprozvanny and Maximov, 2001) suggest two positions in PDZ domains as determining their binding specificities. 'Pos1' is the first residue after the βB strand, and 'Pos2' is the first residue in the βA helix. The authors have determined 5 groups for Pos1 and five groups for Pos2, giving a total of 25 PDZ classes. However, the limited experimental data allows to find examples for only 9 out of the 25 classes. In a more recent attempt to classify PDZ domains, Kang *et al.* define three sites in the PDZ domains (S_0, S_{-1} and S_{-2}) (Kang *et al.*, 2003a) where the last 3 carboxy-terminal residues of the peptide ligand bind (P_0, P_{-1} and P_{-2} corresponding to the last, penultimate and antepenultimate residues, respectively). The authors determine five groups of PDZ-ligand complexes depending on the combination of occupied S sites by the ligand. These combinatorial models even include models for non C-terminal ligands.

Finally, this classification is supported and extended by the observations made by Walma, which led to a new system of classification (Walma, 2004). She showed that two classes are distinguishable, depending on the solvent accessibility of only one residue in the ligand, P_{-1}, giving an unprecedented importance to that residue in PDZ-ligand complex formation. When P_{-1} is highly buried (>80%) in the PDZ domain upon binding, the ligand is called a P1 type of ligand. When P_{-1} is less buried (<75%), the ligand is a P2 type. For each type of ligand, specific regions in the PDZ fold were identified that interact with the residues of the ligand up to P_{-3} (see

Table 1.1). Namely, P$_{-1}$ residues of the P1 type of ligand make contact with residues at the C-terminus of βC and L1, while the P$_{-1}$ residues of P2 types of ligand interact with only one residue at the N-terminus of the βB strand. Furthermore, the P$_{-2}$ residues of P1 type of ligands do not show specific interactions with their PDZ partners, while the P$_{-2}$ residues of P2 type of ligands show interactions with residues placed in the αB helix of the PDZ domain. Finally, the P$_{-3}$ residues of P1 type of ligands interact with the N-terminus of the βB strand, while the P$_{-3}$ residues of P2 type of ligand make contact with the C-terminus of βB and N-terminus of the αB helix.

Table 1.1: Typical interaction of PDZ domain regions with the P$_{-1}$, P$_{-2}$ and P$_{-3}$ residues of P1 and P2 types of ligands.

	P1 type of ligand	P2 type of ligand
P$_{-1}$ residue	C-terminus of βC strand, loop L1	N-terminus of βB strand
P$_{-2}$ residue	-	αB helix
P$_{-3}$ residue	N-terminus of βB strand	C-terminus of βB strand, N-terminus of αB helix

In another view, PDZ domains are not considered isolated items within the protein. Rather, they appear to be working in tandem. The rationale behind this phenomenon is not yet understood. Some studies report a cooperative mechanism, while others show that a combination of PDZ domains improves the stability of their three dimensional folds (Grootjans *et al.*, 2000; Feng *et al.*, 2003; Long *et al.*, 2003), although this does not seem to be universal (Kang *et al.*, 2003b).

I.5 - OVERVIEW OF THIS THESIS

The goal of this research was to examine the interaction between the third domain of the human CCS (CCSIII) and the second PDZ domain of X11α (PDZ2α).

Among the 40 residues of the human CCSIII, there are two potential binding sites, one at the C-terminus, and the other in the middle of CCSIII. The C-terminal sequence of human CCSIII (AQPPAHL) only partially fits the class II consensus sequence (see section I.4.2), as the antepenultimate P_{-2} residue of CCSIII does not contain the large hydrophobic residue but an alanine instead. Alternatively, the residues $G^{248}LTIWEER^{255}$ of CCSIII could present an internal interaction motif in analogy of the syntrophin-NOS complex.

Using high-resolution NMR spectroscopy the structural basis of the interaction between CCSIII and PDZ2α was examined. The resonance frequencies of most ^{1}H, ^{15}N and ^{13}C nuclei of PDZ2α were determined (Chapter 2). These were then used to solve the structure of PDZ2α in solution (Chapter 3). We then explored the binding of the C-terminal and internal CCSIII sequence motifs, and interpreted the results using the structure of PDZ2α (Chapter 4).

The results presented so far were done on a tagged protein. Ideally, one would prefer to work on untagged protein for the type of research that has been done here. Thus, the possibility of separating tags from a protein of interest with a new generation of proteases, Pd compounds, was investigated. The results are reported in Chapter 5.

In Chapter 6, a general discussion of the results is provided.

Chapter II

^{1}H, ^{13}C, and ^{15}N assignment of the second PDZ domain of the neuronal adaptor protein X11α

II.1 - INTRODUCTION

Copper is an important cofactor of a number of proteins involved in essential biological reactions. As copper ions are highly reactive in solution, nature has devised systems to avoid free copper ions in the cell (Rae *et al.*, 1999). One example of such a system is the couple CCS–SOD1. CCS presumably takes the Cu^+ from one of the copper transporters at the plasma membrane and brings it to the cytoplasmic SOD1 (Culotta *et al.*, 1997). A functional CCS is necessary for SOD1 to acquire Cu^+ and be active. McLoughlin *et al.* have demonstrated that CCS can interact with a neuron protein (X11α) via their C-terminal (CCSIII) and second PDZ domains (PDZ2α), respectively (McLoughlin *et al.*, 2001), with an inactive SOD1 as a result.

X11α is a so-called adaptor protein; via its various domains, it forms multi-protein complexes that are involved in signal transduction and cellular communication (Okamoto and Sudhof, 1997; Butz *et al.*, 1998; Biederer *et al.*, 2002; Ho *et al.*, 2002).

PDZ domains are commonly described as cellular glues, enhancing the formation of complexes of proteins involved in signal transduction (Fanning and Anderson, 1999; van Ham and Hendriks, 2003).

In view of the above-mentioned interaction between CCSIII and PDZ2α, McLoughlin *et al.* suggest a new role for X11α and PDZ domains.

The above mentioned interaction between PDZ2α and CCSIII constitutes thus a new type of interaction. Determination of the structure of PDZ2α and of its complex with (part of) CCSIII may give new insights into how the interaction between X11α and CCS affects the loading of SOD1 with copper. The first step toward structure calculation by NMR is the assignment of the NMR spectra of PDZ2α, which is presented in this chapter.

II.2 - MATERIALS AND METHODS

II.2.1 - Protein expression and purification:

The sequence coding from residue 745 to 823 of X11α (corresponding to our residues 12 to 90) (see Figure 2.1) was cloned by PCR from human brain cDNA into a pET3H expression vector (Chen and Hai, 1994), resulting in a construct with an N-terminal poly-histidine tag and 6 additional residues (LETMGN) in front of the original PDZ sequence. The gene was over-expressed in *E.coli* BL21 (DE3*RP) grown at 28°C. For full isotope labeling, M9 minimal medium was supplemented with $^{15}NH_4Cl$ (0.5 g/L) and uniformly labeled ^{13}C-glucose (3 g/L) (CIL, Andover MA) as sole sources of nitrogen and carbon. For the purpose of stereospecific assignment, M9 minimal medium was supplemented with $^{15}NH_4Cl$ (0.5 g/L), 10% uniformly labeled ^{13}C-glucose (0.5 g/L) and 90% unlabeled glucose (4.5 g/L) (Senn *et al.*, 1989). When the OD_{600} of the culture reached 0.6, expression was induced by adding 0.5 mM IPTG and incubation was continued for 11 hours. After centrifugation, the cell pellet of 1 L of culture was resuspended in 10 ml 20 mM Tris-HCl pH 8.0 and kept at -80°C until the next step. After thawing, the cells were sonicated in the presence of 1 mM PMSF and 0.1% NP-40 (a non-ionic detergent). The lysate was brought to 0.5 M NaCl prior to centrifugation at 30,000 g for 1 hour. The supernatant was then loaded onto a Hi-Trap Chelate resin (Pharmacia) saturated with nickel and eluted with an imidazole gradient (0 to 400 mM in 20 mM Tris, 0.5 M NaCl, pH 8.0). The eluted fractions were analyzed on 15% PAA Tris/Tricine/SDS gel. Those exhibiting a single band on the gel below 14 kDa were pooled and dialyzed extensively against MilliQ grade water. Precipitates were removed by centrifugation for 10 minutes at 4500g.

II.2.2 - NMR spectroscopy:

For NMR analysis the purified PDZ2α domain was concentrated by evaporation in a centrifuge under vacuum to ca. 2.2 mM in 250 μl and brought to 10 mM sodium phosphate buffer pH 6.7. A deuterated sample was obtained (where the labile protons were exchanged for deuterium) by a series of concentrations-dilutions in

D$_2$O; subsequently, the sample was brought to 10 mM sodium phosphate buffer (in D$_2$O) pH 6.7 (uncorrected for deuterium effect). Sequence specific assignments of ^{13}C$_\alpha$, ^{13}C$_\beta$, ^{13}CO, ^{15}N and HN were obtained from HNCACB, HNCO and HN(CA)CO experiments. Aliphatic assignments for the side chains were obtained from H(CCCO)NH, CCCONH, CCH and HCCH-TOCSY experiments. This set of spectra was recorded on a Bruker DMX 600 MHz spectrometer at 290K equipped with a TXI-Z-GRAD (^{1}H, ^{15}N, ^{13}C) probe. The data were processed using the Azara 2.7 suite of programs, provided by Wayne Boucher and the Department of Biochemistry, University of Cambridge (available at www.bio.cam.ac.uk). They were further analyzed with Ansig for Windows (Helgstrand *et al.*, 2000). The aromatic carbons and protons were assigned from CBCDHD and CBCDHE spectra. Stereospecific assignments of valine and leucine side chain methyls were obtained from ^{13}C-CT-HSQC experiments using a 10% ^{13}C-labeled sample brought to a concentration of 2.5 mM in 250 µl.

This set of data was recorded on a Varian Unity Inova 600 at 290 K and was processed with NMRPipe suite (Delaglio *et al.*, 1995) (see http://spin.niddk.nih.gov/bax/software/NMRPipe/).

II.3 - RESULTS

II.3.1 - *Purification of PDZ2α*

The PDZ2α domain consists of a six-histidine-tag, followed by an engineered linker of six residues (LETMGN), and then residues 745 to 823 of the original X11α sequence (corresponding to residues 12 to 90 in our numbering – see Figure 2.1 and the Material and Methods section of this chapter).

```
                     753           763           773           783
0            10        20            30            40            50
HHHHHHLETMG NVTTVLIRRP DLRYQLGFSV QNGIICSLMR GGIAERGGVR

                     793           803           813           823
             60        70            80            90
 VGHRIIEING QSVVATPHEK IVHILSNAVG EIHMKTMPAA
```

Figure 2.1: Sequence of the PDZ2α construct. The numbers in bold correspond to the Swiss-Prot numbering (accession code Q02410). The numbers in italics correspond to the numbering used throughout this manuscript. The underlined bold residues indicate the conserved arginine coordinating the ligand via a water molecule, and the conserved binding motif.

The purification of PDZ2α is straightforward. One step of nickel-IMAC (Immobilized Metal Affinity Chromatography) suffices to eliminate almost all contaminating *E.coli* proteins. The remaining contaminants precipitate during dialysis against MilliQ water (see Figure 2.2) and are removed by centrifugation, leading to a fraction of PDZ2α over 95 % pure. One liter of bacterial culture in M9 minimal medium yield about 10 mg of PDZ2α.
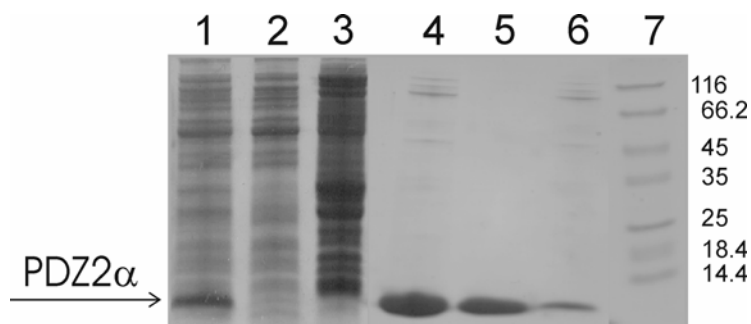
Figure 2.2: Purification of PDZ2α. (1) Soluble fraction of *E.coli* after sonication and centrifugation; (2) Non-binding fraction; (3) Fraction of non specifically bound proteins, eluted at 30 mM imidazole; (4) Fraction of specifically bound proteins, eluted at 120 mM imidazole; (5) Soluble PDZ2α after dialysis against water;(6) Insoluble fraction after dialysis; (7) Standard molecular weight marker. The molecular masses are indicated at the right hand side of the gel in kDa.

II.3.2 - Extent of assignment and data deposition

The ¹⁵N-HSQC spectrum of PDZ2α at pH 6.7 and 290 K is shown in Figure 2.3. The backbone ¹H, ¹⁵N, ¹³C$_\alpha$ and ¹³CO have been completely assigned except for the N-terminal His-tag, Leu 6 and Pro 67. All aliphatic side chain protons have been fully assigned except for Leu 75. All protonated ¹³C and ¹⁵N resonances are available except for some histidine aromatic rings (H53, H68, H73 and H83), the side chain methyls of methionines (M9, M39, M84 and M87). Of all arginines in the PDZ2a sequence, only the ¹⁵N$_\varepsilon$'s of Arg 19 and 54 were determined.
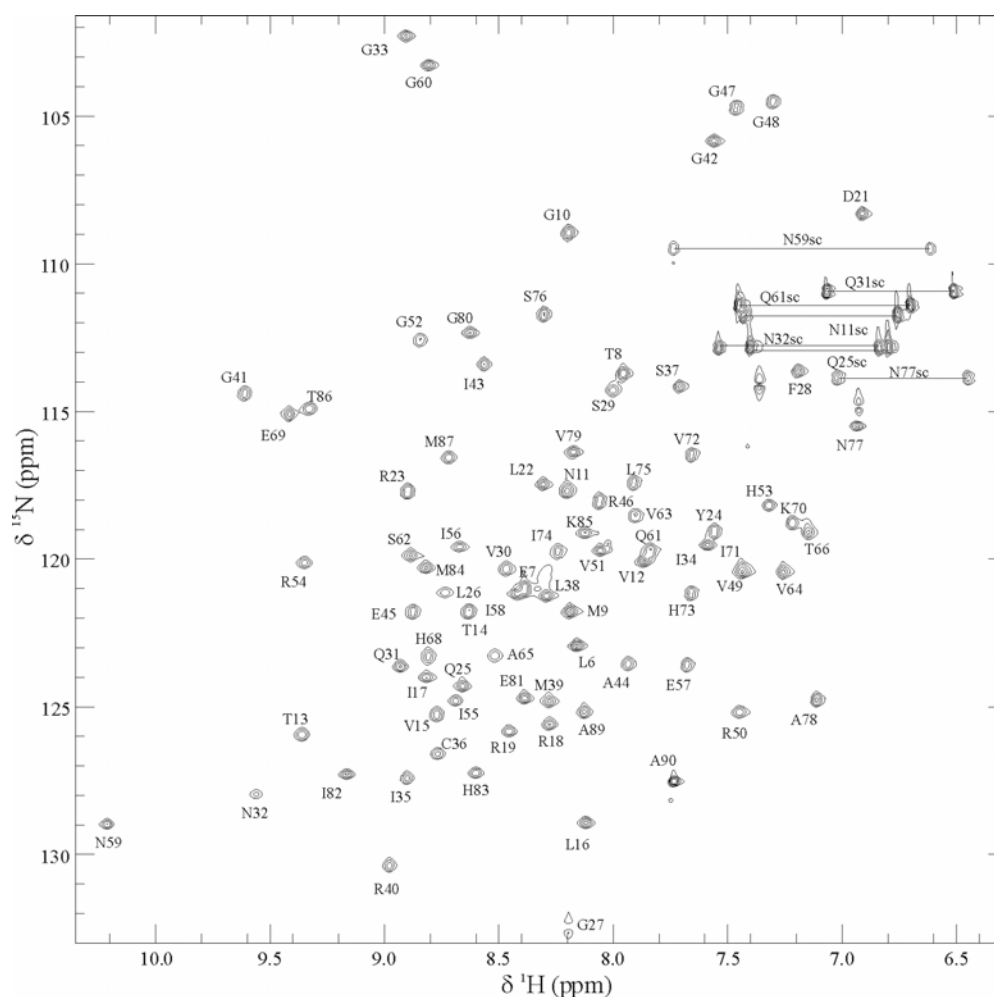
Figure 2.3: 600 MHz [15N,1H]-HSQC spectrum of 2.2 mM uniformly ¹³C, ¹⁵N-labeled PDZ2α in 10mM sodium phosphate buffer pH 6.7 at 290K. Resonances are labeled with residue type and sequence number. Side chain amides (sc) are connected by solid lines.

Chemical Shift Index analysis (Wishart and Sykes, 1994) suggests the presence of 4 β-strands (residues 12-18, 28-30, 55-58, and 82-87) and 2 α-helices (residues 43-46, and 68-76) in PDZ2α (see Figure 2.4). This prediction is in agreement with the known structures of other PDZ domains.
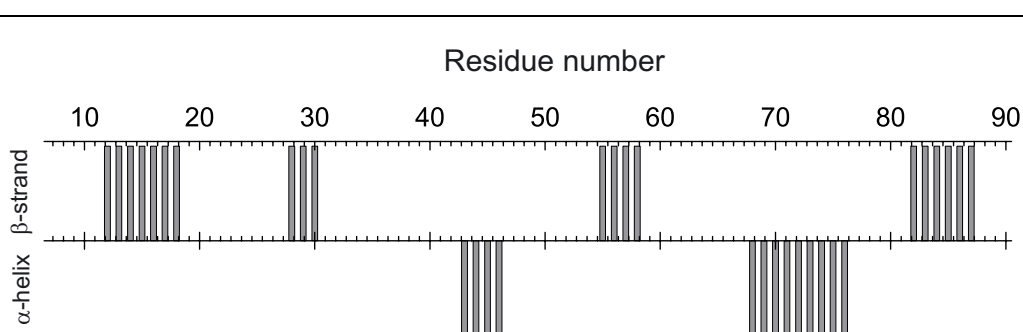
Figure 2.4: Secondary structure prediction of PDZ2α based on the chemical shift index (CSI) (Wishart and Sykes, 1994).

The assignments as presented in Table 2.1 have been deposited at the BMRB, under accession number 6113.

The assignment list is sufficiently complete to proceed with structure determination protocols (see Chapter 3).

Table 2.1: Assignment table of PDZ2α

Residue	Backbone N (HN)	CO	Cα (Hα)	Cβ (Hβ)	others
Glu 7	120.8 (8.32)	176.6	56.4 (4.06)	29.7 (1.73,1.83)	CG 36.0 (2.23) CD-
Thr 8	113.6 (7.91)	174.5	61.5 (4.11)	69.2 (3.99)	CG2 21.2 (1.16)
Met 9	121.4 (8.13)	176.3	55.2 (4.26)	32.3 (1.78,1.88)	CG 31.8 (2.38,2.29) CE-
Gly 10	108.6 (8.12)	173.3	43.0 (3.91)		
Asn 11	117.2 (8.13)	174.5	52.7 (4.48)	38.2 (2.51,2.58)	CG- ND2 111.3 (6.67,7.35)
Val 12	119.7 (7.80)	176.3	61.6 (4.29)	33.0 (1.80)	CG1 21.6 (0.90) CG2 21.2 (0.91)
Thr 13	125.6 (9.28)	173.1	62.3 (4.28)	70.1 (4.01)	CG2 20.9 (1.03)
Thr 14	121.4 (8.56)	173.1	60.2 (4.56)	69.2 (3.85)	CG2 21.4 (1.17)
Val 15	124.8 (8.70)	173.9	59.7 (4.23)	35.0 (1.50)	CG1 21.3 (0.63) CG2 20.4 (0.60)
Leu 16	128.5 (8.05)	174.9	54.1 (4.75)	43.4 (1.11,1.41)	CG 27.4 (0.83) CD1 23.6 (0.45) CD2 24.0 (0.58)
Ile 17	123.2 (8.71)	173.7	59.1 (4.08)	40.7 (1.44)	CG1 26.6 (1.25,0.66) CG2 13.8 (0.73) CD1 17.5 (0.72)
Arg 18	124.7 (8.17)	173.6	52.7 (4.47)	30.1 (1.52)	CG 28.0 (1.16,0.99) CD 42.6 (3.06) CZ- NE- NH1- NH2-
Arg 19	125.0 (8.35)	173.1	51.9 (4.36)	32.5 (1.07,1.66)	CG 27.0 (1.39,1.17) CD 44.4 (2.71,3.33) CZ- NE 131.3 (6.83) NH1- NH2-
Pro 20		175.7	65.5 (3.84)	32.3 (1.51,2.08)	CG 26.7 (1.45,1.32) CD 49.4 (3.44)
Asp 21	108.1 (6.83)	175.3	52.8 (4.29)	42.4 (2.63,2.75)	CG-
Leu 22	117.2 (8.24)	177.3	56.3 (3.82)	41.1 (1.40,1.48)	CG 26.3 (1.40) CD1 24.7 (0.90) CD2 22.6 (0.71)
Arg 23	117.3 (8.80)	177.5	57.1 (3.86)	29.1 (1.48,1.65)	CG 26.5 (1.53) CD 42.9 (2.83,2.94) CZ- NE- NH1- NH2-
Tyr 24	118.5 (7.46)	175.5	57.2 (4.15)	38.2 (2.71,2.86)	CG- CD1/CD2 132.8 (7.06) CE1/CE2 118.2 (6.68) CZ-
Gln 25	123.5 (8.55)	176.4	55.0 (4.05)	28.5 (1.71,1.97)	CG 33.5 (2.39) CD- NE2 112.2 (6.68,7.31)
Leu 26	120.0 (8.30)	177.4	56.8 (3.76)	41.7 (1.03,1.30)	CG 15.6 (1.40) CD1 25.4 (0.77) CD2 22.7 (0.71)
Gly 27	132.4 (8.19)	174.5	46.0 (3.62,4.02)		
Phe 28	113.6 (7.16)	172.3	55.7 (4.94)	40.0 (2.90,3.14)	CG- CD1/CD2 132.3 (6.80) CE1/CE2 129.8 (6.66) CZ 128.0 (6.71)

Table 2.2 (continued)

Residue	Backbone N (HN)	CO	Cα (Hα)	Cβ (Hβ)	others
Ser 29	113.6 (7.93)	172.6	54.2 (4.69)	65.4 (3.66)	
Val 30	119.8 (8.42)	174.3	58.9 (5.03)	35.3 (1.58)	CG1 21.0 (0.82) CG2 21.1 (0.79)
Gln 31	123.3 (8.83)	175.6	52.6 (4.22)	28.4 (2.13)	CG 31.1 (1.93) CD- NE2 110.4 (6.44,6.98)
Asn 32	127.8 (9.49)	174.6	54.0 (4.12)	36.7 (2.62,2.87)	CG N D2 112.4 (6.75,7.46)
Gly 33	126.5 (8.83)	171.4	45.3 (3.02,4.12)		
Ile 34	119.1 (7.50)	176.1	58.6 (4.48)	38.6 (1.69)	CG1 27.5 (1.34,0.70) CG2 16.5 (0.68) CD1 12.0 (0.79)
Ile 35	126.9 (8.79)	176.2	61.9 (4.22)	36.9 (1.89)	CG1 27.6 (1.42,0.74) CG2 18.2 (0.79) CD1 13.5 (0.58)
Cys 36	126.2 (8.68)	173.5	55.9 (4.67)	29.6 (2.53,2.80)	
Ser 37	113.5 (7.60)	171.4	57.6 (4.23)	63.9 (3.57,3.60)	
Leu 38	120.7 (8.23)	175.4	53.7 (4.62)	46.3 (1.03,1.35)	CG 26.2 (1.12) CD1 24.6 (0.79) CD2 26.0 (0.75)
Met 39	124.1 (8.16)	176.3	54.5 (4.23)	32.6 (1.73,1.80)	CG 31.2 (2.32,2.23) CE-
Arg 40	130.0 (8.90)	178	56.9 (3.98)	28.8 (1.81)	CG 26.3 (1.58,1.41) CD 42.5 (3.24) CZ- NE- NH1- NH2-
Gly 41	114.2 (9.53)	174.6	45.1 (3.55,3.93)		
Gly 42	130.1 (7.48)	174	44.3 (3.80,4.20)		
Ile 43	113.4 (8.51)	178.6	64.9 (3.65)	37.2 (1.80)	CG1 26.2 (1.41,1.24) CG2 17.8 (1.12) CD1 13.6 (0.94)
Ala 44	122.9 (7.93)	178.4	54.4 (3.81)	18.3 (1.37)	
Glu 45	121.2 (8.81)	180.6	59.4 (3.70)	29.4 (1.86,1.97)	CG 36.5 (2.01,1.94) CD-
Arg 46	117.7 (7.98)	177.4	58.4 (3.87)	29.8 (1.87)	CG 27.5 (1.55,1.48) CD 43.0 (2.94,2.99) CZ- NE- NH1- NH2-
Gly 47	128.9 (7.40)	173.2	45.0 (3.32,4.16)		
Gly 48	128.7 (7.21)	174.5	44.5 (3.37,4.10)		
Val 49	119.9 (7.35)	174	63.6 (3.16)	30.2 (1.02)	CG1 22.2 (0.25) CG2 23.7 (0.45)
Arg 50	124.7 (7.39)	174.8	52.9 (4.12)	31.0 (0.10,0.92)	CG 26.0 (1.24) CD 42.6 (2.57,2.66) CZ- NE- NH1- NH2-

Table 2.3 (continued)

Residue	Backbone N (HN)	CO	Cα (Hα)	Cβ (Hβ)	others
Val 51	119.2 (7.96)	176.8	63.3 (3.22)	31.2 (1.63)	CG1 20.8 (0.84) CG2 22.7 (0.86)
Gly 52	112.2 (8.75)	174.1	44.6 (3.44,4.16)		
His 53	117.7 (7.22)	174	32.3 (4.68)	33.8 (2.53,2.99)	CG- CD2 114.2 (6.52) CE1 (6.52) ND1- NE2-
Arg 54	119.6 (9.25)	175.9	53.6 (4.75)	32.4 (1.62)	CG 26.8 (1.31,1.14) CD 42.7 (2.85,3.08) CZ-NE 130.9 (7.27) NH1- NH2-
Ile 55	124.4 (8.61)	174.7	62.3 (3.76)	38.6 (1.40)	CG1 27.3 (1.76) CG2 18.5 (0.82) CD1 14.5 (0.83)
Ile 56	119.0 (8.58)	176.9	60.6 (4.31)	38.6 (1.66)	CG1 26.5 (1.20) CG2 17.4 (0.80) CD1 13.1 (0.75)
Glu 57	123.4 (7.60)	174.5	55.4 (4.99)	35.5 (1.52,1.67)	CG 36.9 (1.67,1.59) CD-
Ile 58	120.8 (8.33)	175.7	60.6 (4.51)	40.9 (1.37)	CG1 127.4 (1.33,0.67)- CG2 16.5 (0.75) CD1 14.4 (0.87)
Asn 59	128.6 (10.13)	175.3	53.8 (4.37)	36.5 (2.59,2.96)	CG- ND2 109.0 (6.52,7.65)
Gly 60	127.5 (8.73)	173.1	44.9 (3.35,3.87)		
Gln 61	119.3 (7.75)	174.8	53.2 (4.32)	29.6 (1.78,1.89)	CG 32.8 (2.11,2.03) CD- NE2 111.0 (6.62,7.37)
Ser 62	119.4 (8.81)	176.9	58.3 (4.44)	62.5 (3.62,3.88)	
Val 63	118.1 (7.81)	176.6	59.4 (5.03)	30.8 (2.28)	CG1 20.1 (0.80) CG2 18.5 (0.48)
Val 64	120.0 (7.17)	175.9	64.6 (3.73)	31.6 (1.84)	CG1 20.8 (1.01) CG2 20.8 (1.06)
Ala 65	122.9 (8.44)	176.5	50.8 (4.33)	18.0 (1.34)	
Thr 66	118.7 (7.06)	171.4	60.7 (4.31)	70.2 (3.68)	CG2 21.8 (1.35)
Pro 67		-	62.5 (4.21)	32.7 (1.75,2.33)	
His 68	122.8 (8.72)	176.6	60.0 (3.99)	31.6 (2.86,3.20)	CG- CD2- (6.78) CE1- ND1- NE2-
Glu 69	114.6 (9.34)	178.6	59.3 (3.53)	28.2 (2.01)	CG 36.1 (2.37) CD-
Lys 70	118.4 (7.13)	178	57.6 (4.05)	31.5 (1.88)	CG 24.7 (1.26,1.22) CD 28.3 (1.44,1.50) CE 41.6 (2.93) NZ-
Ile 71	119.9 (7.35)	177.2	66.2 (3.26)	37.3 (1.70)	CG1 29.6 (1.52,0.47) CG2 16.4 (0.78) CD1 13.1 (0.96)
Val 72	116.0 (7.58)	178.4	66.4 (3.16)	31.0 (1.65)	CG1 20.7 (0.80) CG2 21.8 (0.60)

Table 2.4 (continued)

Residue	Backbone N (HN)	CO	Cα (Hα)	Cβ (Hβ)	others
His 73	120.8 (7.58)	177.9	60.3 (3.95)	30.4 (2.99,3.07)	CG- CD2- (6.72) CE1- ND1- NE2-
Ile 74	119.1 (8.15)	179.4	64.9 (3.38)	38.3 (1.66)	CG1 28.5 (1.76,0.85) CG2 16.9 (0.85) CD1 13.6 (0.79)
Leu 75	117.0 (7.83)	178	57.3 (3.69)	41.6 (1.05,1.58)	CG 25.9 (0.57) CD1- CD2 22.5 (0.88)
Ser 76	111.2 (8.22)	175.1	60.8 (4.01)	62.7 (3.62,3.66)	
Asn 77	114.8 (6.82)	173.3	53.5 (4.52)	40.4 (2.12,2.48)	CG -ND2 113.6 (6.37,6.94)
Ala 78	124.3 (7.01)	175.2	52.4 (4.14)	17.5 (1.38)	
Val 79	116.1 (8.12)	174.4	59.8 (4.16)	35.7 (1.74)	CG1 20.5 (0.78) CG2 19.5 (0.83)
Gly 80	111.9 (8.51)	173.5	44.7 (3.21,3.91)		
Glu 81	124.1 (8.31)	175.3	55.7 (4.13)	29.4 (1.38,1.76)	CG 36.5 (2.05,1.70) CD-
Ile 82	127.0 (9.08)	174.3	60.6 (4.17)	38.7 (1.52)	CG1 26.2 (1.45) CG2 16.2 (0.63) CD1 14.9 (0.65)
His 83	126.8 (8.50)	175.7	54.3 (4.93)	31.8 (2.81,2.95)	CG- CD2- (6.79) CE1- ND1- NE2-
Met 84	119.9 (8.74)	174.5	53.7 (5.23)	38.0 (1.55,1.84)	CG 31.2 (2.25,2.06) CE 15.6 (1.60)
Lys 85	118.6 (8.04)	176	54.5 (5.38)	35.6 (1.29,1.36)	CG 25.3 (1.36) CD 29.0 (1.15,1.35) CE 41.8 (2.71,2.66) NZ -
Thr 86	114.4 (9.25)	171.7	59.4 (5.30)	69.5 (4.22)	CG2 20.1 (0.91)
Met 87	116.1 (8.63)	171.4	53.1 (4.75)	35.2 (1.67,1.77)	CG 30.3 (2.19,2.15) CE-
Pro 88		176.1	63.1 (3.58)	31.3 (1.56,1.94)	CG 27.3 (1.81,1.48) CD 49.7 (3.26,3.30)
Ala 89	124.8 (8.05)	175.6	52.4 (4.01)	19.3 (1.38)	
Ala 90	127.1 (7.65)	181.8	53.0 (3.90)	20.1 (1.29)	

Chapter III

Structure determination of the second PDZ domain of the neuronal adaptor X11α by NMR

ABSTRACT

X11α is a neuron specific multidomain protein involved in protein-protein interactions that mediate signal transduction and cellular communication. A new partner for X11α was discovered, the copper chaperone for superoxide dismutase 1 (CCS), by McLoughlin *et al.* (McLoughlin *et al.* (2001) *J. Biol. Chem.*, **276**, 9303-9307). The interaction was shown to involve the second PDZ domain of X11α (PDZ2α) and the third domain of CCS (CCSIII). In order to study the details of this interaction, the structure of PDZ2α was determined with high-resolution NMR spectroscopy. PDZ2α adopts the canonical PDZ fold with six β-strands and two α-helices. Two special distinguishing features involve the two loops flanking the βB strand: the N-terminal loop is longer while the C-terminal loop is shorter when compared with other known PDZ structures.

III.1 - INTRODUCTION

PDZ domains are commonly referred to as cellular glues. They are present in a large number of proteins, often involved in signal transduction. Their role is to help the formation of protein complexes, usually at the plasma membrane (Fanning and Anderson, 1999; van Ham and Hendriks, 2003). The interaction between the second PDZ domain of X11α (PDZ2α) and the third domain of the copper chaperone for superoxide dismutase (CCSIII) discovered by McLoughlin *et al.* (McLoughlin *et al.*, 2001) suggests a new additional role for PDZ domains.

Despite a low sequence similarity among the PDZ domains, their 3D-structures, consisting of six β-strands and two α-helices, appear remarkably conserved.

The aim of the study is to shed light on the mechanisms of interaction between PDZ2α and CCSIII. The work presented here describes the structure of PDZ2α. The structure was solved by using multidimensional high-resolution NMR spectroscopy.

III.2 - MATERIALS AND METHODS

III.2.1 - Protein expression and purification:

The cloning of the PDZ2α sequence and expression and purification protocols have been described in the Materials and Methods section of Chapter 2.

III.2.2 - NMR spectroscopy:

For NMR analysis the purified PDZ2α domain was concentrated by evaporation in a centrifuge under vacuum to ca. 1.2 mM in 250 μl and brought to 10 mM sodium phosphate buffer pH 6.7. The distance restraints were obtained from 3D ^{15}N-NOESY-HSQC and ^{13}C-NOESY-HSQC spectra, recorded on a Varian Unity Inova 800 MHz spectrometer at 290 K, all with a mixing time of 100 ms. The data were processed with the NMRPipe suite (Delaglio *et al.*, 1995) (http://spin.niddk.nih.gov/bax/software/NMRPipe/) and analyzed with CARA

(Keller, 2004) (available at http://www.nmr.ch/). The T_1, $T_{1\rho}$ and {^{1}H}-^{15}N NOE experiments were recorded on a Varian Unity Inova 600 MHz spectrometer at 290 K. The relaxation delays for the ^{15}N-T_1 experiment were 0.016, 0.096, 0.192, 0.512, 0.768 and 1.024 s. For the ^{15}N-$T_{1\rho}$ experiment they were 0.016, 0.032, 0.048, 0.064, 0.080 and 0.112 s.

III.2.3 - Structure calculation:

The NOE cross-peak assignments and a consistent tertiary fold were obtained from the automated iterative assignment program CANDID (Herrmann *et al.*, 2002), which works in conjunction with three-dimensional structure calculations in the program CYANA (Guntert *et al.*, 1997). The calculations consisted of the standard protocol of seven cycles of iterative NOE assignments and structure calculations (Herrmann *et al.*, 2002). In each of the seven cycles the NOEs assigned by CANDID were supplemented by the backbone dihedral angle constraints obtained from chemical shift analysis using the program TALOS (Cornilescu *et al.*, 1999).

The final structure calculations with CYANA were started from 100 conformers with random torsion angle values. Simulated annealing with 10,000 time steps per conformer was done using the CYANA torsion angle dynamics algorithm (Guntert *et al.*, 1997). Using the FormatConverter, developed as part of the Collaborative Computing Project for the NMR Community (CCPN) (Fogh *et al.*, 2002), the distance and dihedral angle restraints were converted to the X-PLOR (Brünger, 1992) restraint format. Subsequently the 100 generated structures were refined using a short restrained molecular dynamics simulation in explicit solvent (Linge *et al.*, 2003; Nabuurs *et al.*, 2004) in the program XPLOR-NIH (Schwieters *et al.*, 2003). Of these, the 20 lowest energy structures were selected to form the final ensemble.

The quality of the structure ensembles was judged both by their agreement with the experimental restraints and the quality scores as determined by the structure analysis programs PROCHECK (Laskowski *et al.*, 1993) and WHAT_CHECK (Vriend, 1990). Averages and standard deviations were calculated from the checks of the individual members of the final ensemble. The coordinates have been

deposited at the Protein Data Bank, accession code 1Y7N. All figures were made using the program YASARA (http://www.yasara.org/) except for Figures 3.1**B** and 3.1**C** which were made with the program Molmol (Koradi *et al.*, 1996).

III.3 - RESULTS

III.3.1 - Structure of PDZ2α

The solution structure of the second PDZ domain of X11α (PDZ2α) was solved using high-resolution multi-dimensional heteronuclear NMR. The PDZ2α construct consisted of a six-residue histidine-tag, a non-native engineered linker of six residues (LETMGN), followed by residues 745 to 823 of the original X11α sequence (corresponding to residues 12 to 90 in our numbering – see Figure 3.1**A** and the Material and Methods section of Chapter 2). The protein was obtained using the protocol described in Chapter 2. Near-complete assignments of ^{1}H, ^{15}N and ^{13}C spectra were obtained (see Table 2.1) using standard procedures.

On the basis of 1690 NOE-derived distance constraints and 95 dihedral restraints (see Table 3.1) an ensemble of NMR structures was calculated using the torsion-angle dynamics protocol. A tube representation and a stereoview of the ensemble encompassing residues 7 to 90 are shown in Figures 3.1**B** and 3.1**C**, respectively. The ensemble of models has been submitted to the Protein Data Bank (accession code 1Y7N). As expected, the first 6 residues (comprising the His-tag) are not represented because no data were obtained for these residues from the NMR experiments. The ensemble was analyzed using the programs PROCHECK (Laskowski *et al.*, 1993) and WHAT IF (Vriend, 1990), and the structural statistics are reported in Table 3.1. The average pairwise RMSD of the ordered backbone heavy atoms (using residues 14 to 87) is 0.50 ± 0.10 Å, while the average pairwise RMSD of the global backbone heavy atoms is 1.02 ± 0.26 Å, indicating a well-defined ensemble, even in the loop regions. The Ramachandran analysis displays 90.3% of the residues in the most

favored region, and an additional 9.2% in the allowed regions. The average RMS Z-scores are close to 1, indicating a good covalent geometry of the ensemble.

The ensemble displays a compact fold formed of six β-strands (βA to βF), two α-helices (αA and αB), 3 loops and 4 β-turns (L1 to L7) packed in the characteristic PDZ fold. The conserved arginine of the peptide binding motif is situated in the loop L1 and the consensus binding motif is between the loop L1 and the β-strand βB. As expected, the groove for ligand interaction, formed by the second β-strand (βB) and the second α-helix (αB), is also present in PDZ2α. Sequence and structural alignment with the third PDZ domain of Psd-95 (PDB code 1BE9 (Doyle *et al.*, 1996)) and the second PDZ domain of PTP-BL (PDB code 1GM1 (Walma *et al.*, 2002)) (see Figures 3.2**A** and 3.2**B**) shows two unique features for the PDZ2α ensemble. First, the loop L1, connecting the first and the second β-strand, is longer by two residues (Leu 22 and Arg 23), forming a cap above the binding groove. Although this L1-loop is longer, the position of the consensus binding motif (QLGF) remains structurally unchanged at the border between L1 and the second β-strand (βB), allowing the residues Leu 26 and Gly 27 to form the bulge typical for PDZ domains. Second, the loop L2, situated between the second and the third β-strand, consists of only two residues (Asn 32 and Gly 33). It is six to ten residues shorter when compared to most other PDZ domains. However, the positions of the secondary structure elements with respect to each other are not perturbed. Figure 3.2**B** shows that the strands βC to βF and the helix αB align properly on top of their homologues in the other two PDZ domains. Only the helix αA does not align well with its homologue in 1BE9 and 1GM1. The enlargement presented in Figure 3.2**C** shows the side chains of the conserved residues among the three superimposed PDZ domains. The Arg 19 backbone of PDZ2α does not overlap very well with its homologues in the other two PDZ domains because it is situated at the start of the loop L1. However, the side chain of Arg 19 overlaps well with its homologues, pointing inside the binding groove. In the binding motif, three out of four residues (Leu 26, Gly27 and Phe 28) are oriented in a similar way as their homologues in the other two PDZ domains. Only the first residue (Gln 25 in PDZ2α), which is present at the end of loop L1, appears to have different orientations in all three PDZ domains.
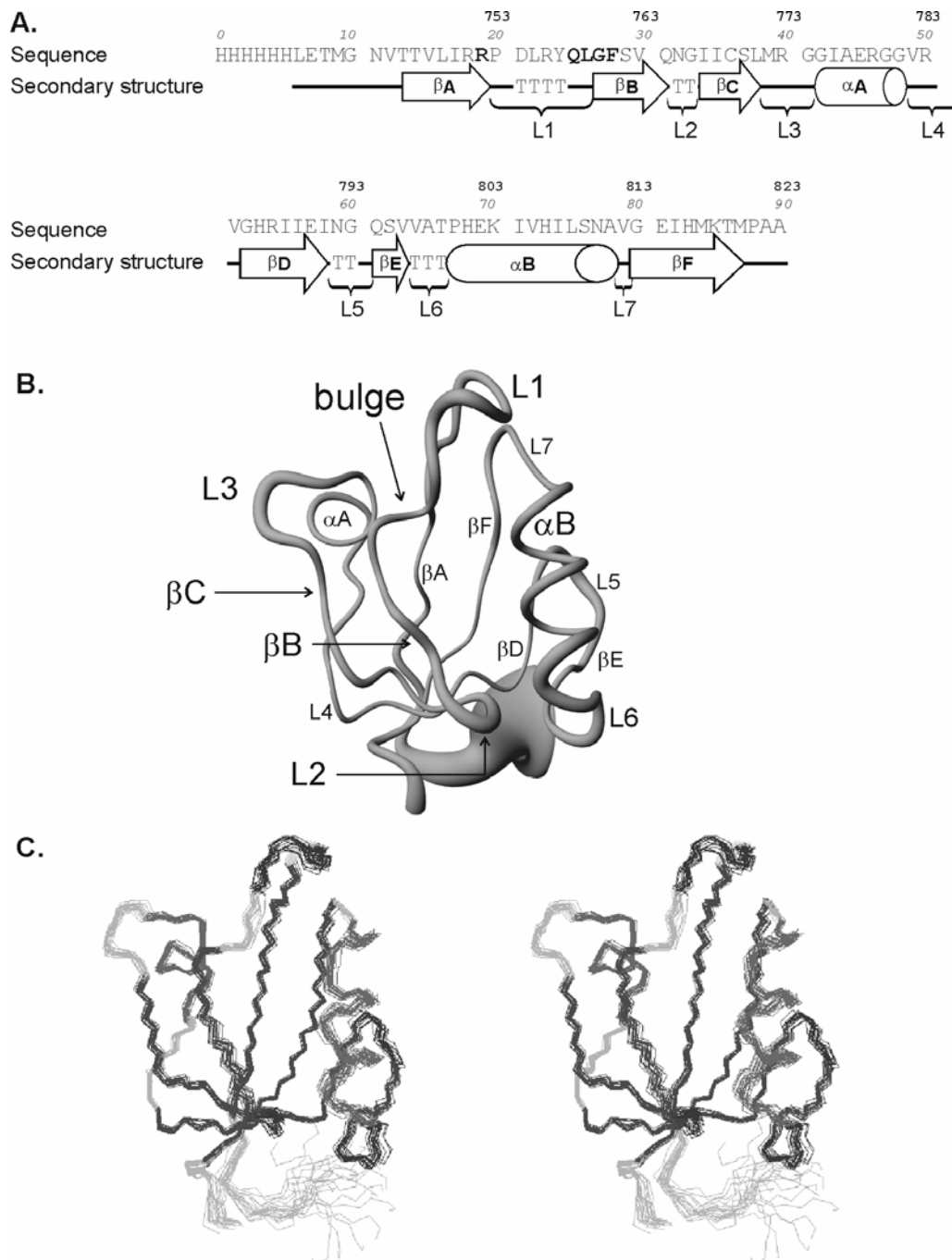
Figure 3.1: A. Sequence of the PDZ2α construct. The numbers in bold correspond to the Swiss-Prot numbering. The numbers in italics correspond to the numbering used throughout this paper The residues in bold indicate the conserved arginine (R19) coordinating the ligand via a water molecule in other PDZ-peptide complexes, and the conserved binding motif (Q25 to F28). The secondary structure elements of PDZ2α are shown below the sequence. T indicates residues in β-turns; **B.** Tube representation of an ensemble of 20 superimposed models of PDZ2α. The diameter of the tube represents the RMSD of the backbone atoms in the ensemble; **C.** Stereoview of the same PDZ2α ensemble as in B. The α-helices, the β-strands and the β-turns are indicated in dark.

Table 3.1: Structural statistics for the ensemble of the 20 best models of the PDZ2α[a]

A. *Restraint information*

Distance restraints	1690
(intra-residual/sequential/medium/long)	(313 / 442 / 324 / 611)
Hydrogen bonding restraints	-
Dihedral angle restraints (phi/psi)	95 (48 / 47)
Structural uncertainty (bits/atom^2, I_{total} / $H_{structure|R}$)[b]	1.911 / 4.359
Information distribution (%, dihedral/intra-residual/sequential/medium/long)[b]	1.1 / 0.2 / 0.7 / 15.0 / 83.0

B. *Average RMS deviation from experimental restraints*

Distance restraints (Å)	0.021 ± 0.001
Dihedral angle restraints (deg.)	0.32 ± 0.08

C. *Average Pairwise Cartesian RMS deviation (Å)*

Global backbone heavy atoms	1.02 ± 0.26
Global all heavy atoms	1.65 ± 0.22
Ordered backbone heavy atoms	0.50 ± 0.10
Ordered all heavy atoms	1.22 ± 0.13

D. *Ramachandran quality parameters (%)*[d]

Residues in favored regions	90.3
Residues in allowed regions	9.2
Residues in additionally allowed regions	0.4
Residues in disallowed regions	0.1

E. *Average RMS deviation from current reliable structures (RMS Z-scores, null deviation=1)*[e]

Bond lengths	0.97
Bond angles	0.83
Omega angle restraints	0.60
Side-chain planarity	0.98
Improper dihedral distribution	0.78
Inside / outside distribution	0.98

F. *Average deviation from current liable structures (Z-scores, null deviation=0)*[e]

1st generation packing quality	-1.0
2nd generation packing quality	0.3
Ramachandran plot appearance	-2.5
Chi-1 / chi-2 rotamer normality	-1.3
Backbone conformation	-1.9

[a] PDB accession code: 1Y7N
[b] Values calculated using QUEEN (Nabuurs *et al.*, 2003)
[c] Residues involved in secondary structure: 14-87
[d] Values based on PROCHECK (Laskowski *et al.*, 1993) output
[e] Values based on WHATCHECK (Laskowski *et al.*, 1993) output

A.

PDZ2α	11	NVTTVLIRRPDLRYQLGFSVQN----------GIICSLMRGGIAER-GGVRVGHRIIEINGQSVVATPHEKIVHILSNAVGEIHMKTMPA
Psd-95_PDZ3	306	DIPREPRRIVIHRGS--TGLGFNIIGGEDG----EGIFISFILAGGPADLSGELRKGDQILSVNGVDLRNASHEQAAIALKNAGQTVTIIAQYKPEE
PTP-BL_PDZ2	11	GDTFEVELAKTD--GSLGISVTGGVNTSVRHGGIYVKAIIPKGAAESDGRIHKGDRVLAVNGVSLEGATHKQAVETLRNTGQVVHLLLEKQV

B.

C.

Figure 3.2: A. Sequence alignment of PDZ2α (in red, PDZ accession code 1Y7N) with the third PDZ domain of the synaptic protein Psd-95 (in cyan, PDB accession code 1BE9) and the second PDZ domain of the tyrosine phosphatase PTP-BL (in blue, PDZ accession code 1GM1). The arginine (R19) involved in peptide binding is indicated with a "+". The residues of the consensus binding motif are indicated with "-"; **B.** 3D backbone representation of the three aligned PDZ domains mentioned above (same color coding scheme as in A.); **C.** Magnification of the above PDZ domains at the consensus binding region. The side chains of the conserved residues are displayed (same color coding scheme as in A.).

III.3.2 - Dynamics

^{15}N relaxation experiments (({^{1}H}-^{15}N NOE, ^{15}N-R_1 and ^{15}N-$R_{1\rho}$) were recorded on PDZ2α. The resulting data were used to calculate the overall tumbling rate (τ_c), the internal correlation time (τ_e) and the order parameters (S^2) using the model-free approach (Lipari and Szabo, 1982a; Lipari and Szabo, 1982b) (see Figure 3.3) as implemented in the program Modelfree 4.01 (Mandel *et al.*, 1995). Prolines 20, 67 and 88, valine 49 and isoleucines 58 and 71 were not taken into account (because of spectral overlap for the latter three). The overall tumbling rate of PDZ2α is described by an isotropic model with an average global correlation time of 7.1 ± 0.8 ns, which is a typical value for such a small, folded protein at 290 K. The local motion of 38 residues is described by a model incorporating only the S^2 parameter, 31 residues by a model requiring both S^2 and τ_e parameters, and 3 residues by a model with motions on the pico- and sub-nanosecond time scales as described by the S^2, S^2_l and τ_e parameters. Four residues, Arg 19, Val 64, Ala 65 and Thr 66, require a model incorporating chemical exchange, as is also evident from their increased $R_{1\rho}$ relaxation rates. Interestingly, Arg 19 is the conserved residue involved in coordinating a bridging water molecule in the peptide binding pocket. Residues Val 64, Ala 65 and Thr 66 are located in the loop L6, connecting βE and αB. Flexible residues, displaying more pronounced motion on the ps-ns timescale are found at the N-terminal part of βA, the loops L1, L3, L7 and part of βF of PDZ2α.
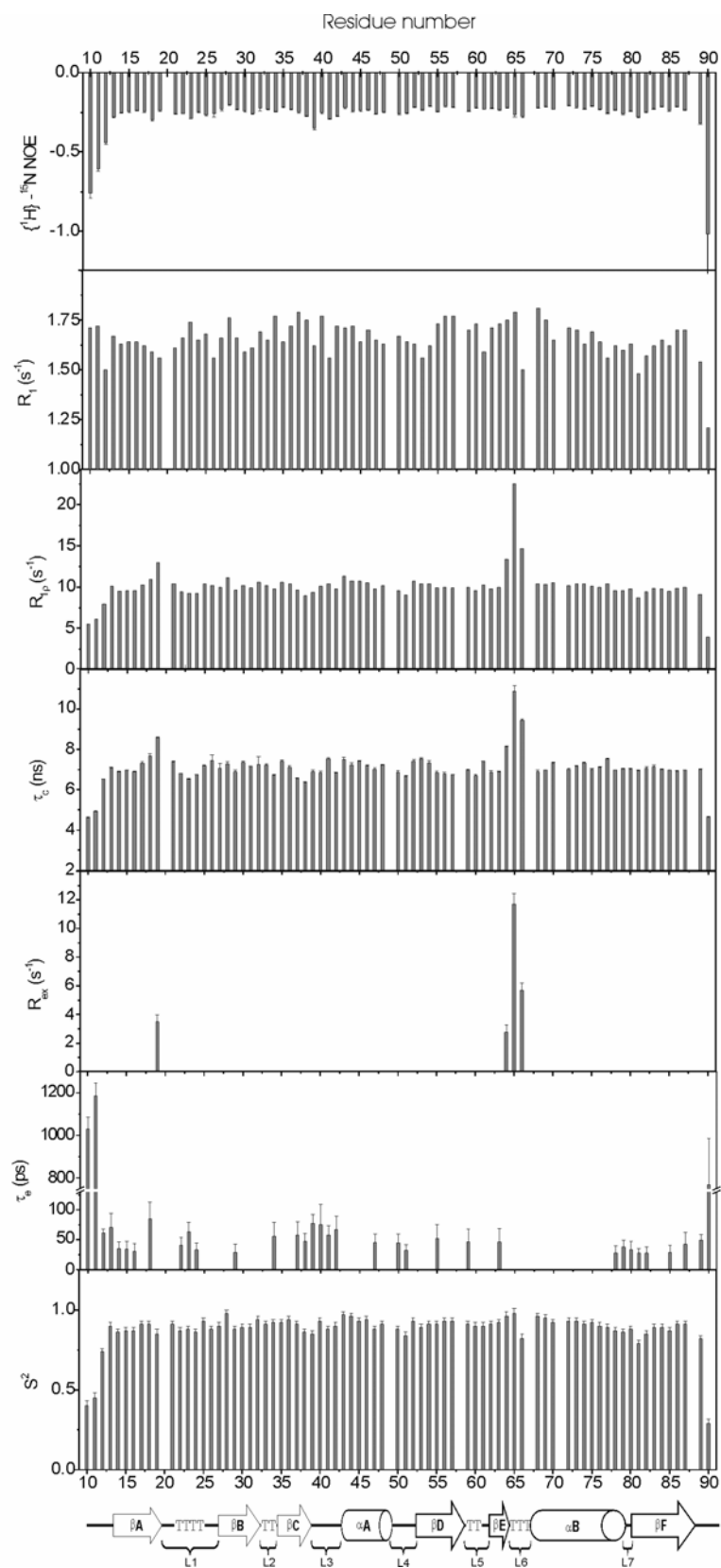
Figure 3.3: [15]N relaxation data (NOE, R_1 and $R_{1\rho}$) and results of the model-free analysis are plotted for all residues. The secondary structure elements are indicated at the bottom.

III.4 - DISCUSSION

The ensemble of 20 superimposed models shows a well-defined structure of PDZ2α. Although the sequence conservation of different PDZ domains is rather low (24% similarity and 14% identity – see Figure 3.2**A**), the PDZ fold is conserved in PDZ2α, with six β-strands and two α-helices.

The structural alignment with the third PDZ domain of Psd-95 (PDB code 1BE9 (Doyle *et al.*, 1996)) and the second PDZ domain of PTP-BL (PDB code 1GM1 (Walma *et al.*, 2002) revealed two special features of PDZ2α (see Figures 3.2**B**): the loop L1 is longer and the loop L2 is shorter. However, the arrangement of the rest of the secondary structural elements with respect to each other is maintained. The conserved residues (Arg 19, Leu 26, Gly 27 and Phe 28) are properly positioned for ligand binding (see Figure 3.2**C**).

Chapter IV

Binding characteristics between the second PDZ domain of X11α and the third domain of CCS.

ABSTRACT

X11α is a neuron specific multidomain protein that interacts with the copper chaperone for superoxide dismutase 1 (CCS) (McLoughlin *et al.* (2001) *J. Biol. Chem.*, **276**, 9303-9307). The authors have demonstrated that the interaction occurs between the second PDZ domain of X11α (PDZ2α) and the third domain of CCS (CCSIII). Two potential binding sites on CCSIII can be distinguished: an internal sequence (G^{248}LTIWEER^{255}) and the C-terminus of CCSIII (AQPPAHL). The interaction was studied by chemical shift perturbation analysis. NMR spectra of the PDZ2α were compared in the absence and in the presence of one of the two peptides mentioned above. No interaction with the internal sequence was observed, while the C-terminal peptide of CCSIII interacts with PDZ2α with a dissociation constant of 91 μM. The results also show that CCSIII does not directly interact with PDZ2α beyond the antepenultimate (P_{-2}) residue of CCSIII (Ala 272).

IV.1 - INTRODUCTION

PDZ domains are cellular glues. Their role is to help the formation of protein complexes, usually at the plasma membrane (Fanning and Anderson, 1999; van Ham and Hendriks, 2003). Despite a low sequence similarity among the PDZ domains, their structures are remarkably conserved, consisting of six β-strands and two α-helices. The classical binding of the carboxy-terminal tail of ligand proteins to PDZ domains occurs in a binding pocket located between βB and αB, creating an extension to the existing β sheet. This interaction involves a conserved sequence motif (G/Q–L–G–F/I) on the PDZ domain and a conserved arginine N-terminal of this motif that is involved in coordination of the carboxy-terminus of the target via a water molecule. The interacting peptides have traditionally been grouped into four classes on the basis of their C-terminal sequences: Class I involves S/TxΦ* sequences (Φ: hydrophobic residue; *: carboxy terminus; x: any residue), Class II involves ΦxΦ*, Class III E/DxΦ* and Class IV VxD/E* sequences (Vaccaro and Dente, 2002). It is now well documented that PDZ domains are promiscuous, and are able to bind C-termini across classes (Palmer *et al.*, 2002; Walma *et al.*, 2002). PDZ domains are also capable of recognizing internal peptide motifs through the very same binding groove (Hillier *et al.*, 1999), such as displayed by the interaction of the second PDZ domain of α1-syntrophin and the C-terminal β-finger of <u>n</u>itrous <u>o</u>xide <u>s</u>ynthase (NOS). Furthermore, PDZ domains have other interaction surfaces (Feng *et al.*, 2002; Feng *et al.*, 2003; Im *et al.*, 2003), and not only proteins but also phospholipids serve as binding targets (Zimmermann *et al.*, 2002).

Among the 40 residues of the human CCSIII, there are two potential binding sites, one at the C-terminus, and the other in the middle of CCSIII. The C-terminal sequence of human CCSIII (AQPPAHL) only partially fits the class-II consensus sequence, as the antepenultimate P_{-2} residue of this motif usually comprises a large hydrophobic residue, instead of the current alanine. Alternatively, the residues G^{248}LTIWEER^{255} could present an internal interaction motif in analogy of the syntrophin-NOS complex.

We have investigated the binding modes between PDZ2α and the two peptides of CCSIII mentioned above, and determined which of the two interacts with PDZ2α. For this purpose, NMR chemical shift perturbation analysis was performed, comparing the backbone resonances of PDZ2α in the absence of any peptide and in the presence of increasing amounts of the peptides. The analysis of the presence/absence of resonance shifts provides information about the residues of PDZ2α involved in peptide binding as well as kinetic data.

IV.2 - MATERIALS AND METHODS

IV.2.1 - Protein expression and purification:

The cloning, expression and purification protocols of PDZ2α were described in the Materials and Methods section of Chapter II.

IV.2.2 - Peptide synthesis:

Synthetic peptides were prepared by solid phase technology on a Syro II peptide synthesizer (MultiSyntech, Witten, Germany) at 10 μmol scale. TentagelS AC or AM resins (Rapp, Tübingen, Germany) were used in combination with Fmoc-protected amino acids carrying TFA-labile side chain protecting groups where needed (Fields and Noble, 1990). Acylations were carried out with a six-fold excess of amino acid using PyBOP/NMM activation in NMP. Deprotection was performed with piperidine/NMP 1/4 (v/v). Cleavage of the peptides and removal of the side chain protecting groups was performed with TFA/water 19/1 (v/v) for 2.5 h at room temperature. Peptides were precipitated with ether/pentane 1/1 (v/v), washed extensively with this mixture and air-dried. Peptides were dissolved in HOAc/water 1/9 (v/v) and lyophilized overnight. RP-HPLC analysis indicated >90% purity and mass spectrometric analysis (Maldi-Tof, Voyager DE Pro, Perseptive Biosystems, Framingham, USA) confirmed the expected molecular masses.

The peptide sequences were as follows: AQPPAHL, Ac-AQPPAHL, Ac-AQPPAHL-NH$_2$, Ac-AQPPAHA, Ac-AQPPAAL, Ac-AQPAAHL, and Ac-GLTIWEER-NH$_2$, wherein 'Ac-' indicates an acetylated N-terminus and '-NH$_2$' indicates an amidated C-terminus.

IV.2.3 - NMR spectroscopy:

For the titration experiments, a solution of the PDZ2α domain was concentrated to 1 mM in 500 μl and brought to 10 mM sodium phosphate buffer pH 6.7. Spectra were recorded on a Bruker DMX 600 MHz spectrometer at 290 K equipped with a TXI-Z-GRAD (^{1}H, ^{13}C, ^{15}N) probe. 2D ^{1}H,^{15}N-HSQC spectra were recorded at each titration point. The data were processed using the Azara 2.7 suite of programs (available at www.bio.cam.ac.uk/azara) and were further analyzed with Ansig for Windows (Helgstrand *et al.*, 2000).

IV.2.4 - Peptide titration:

Each peptide was dissolved in 10 mM sodium phosphate buffer 5% D$_2$O, and the pH was brought to 6.7 by adding concentrated NaOH. The concentrations of the peptide solutions were measured by NMR with 1D single scan experiments. The area under the leucine or alanine methyl resonances was integrated and compared with that of a known standard. Binding curves were obtained by plotting the chemical shift difference ($\Delta\delta^{15}$N) of the backbone nitrogen of the most affected residues against the corresponding peptide:protein ratio (R). The dissociation constant (K$_D$) was derived by global fitting with the following equation (Kannt *et al.*, 1996) in the programme Origin 7.5 (OriginLab Corporation, Northampton, MA):

$$\Delta\delta = \frac{\Delta\delta_{max}\left(T - \sqrt{T^2 - 4R}\right)}{2},$$

where

$$T = 1 + R + \frac{K_D\left([R*A] + B\right)}{A*B},$$

A is the starting concentration of PDZ2α, B the concentration of the stock solution of peptide, and Δδ $_{max}$ the Δδ at R→∞.

The average chemical shift values (Δδ$_{avg}$) were calculated by using the following equation derived (Garrett *et al.*, 1997):

$$\Delta\delta_{avg} = \sqrt{\frac{\left(\frac{\Delta\delta^{15}N}{5}\right)^2 + \left(\Delta\delta^1H\right)^2}{2}} \ ,$$

where Δδ^{15}N and Δδ^{1}H are the chemical shift differences for the backbone nitrogen and proton of a given residue, respectively.

IV.3 - RESULTS

To test the interactions between PDZ2α and CCSIII, the two potential interaction motifs of CCSIII were examined. Peptide 1, derived from the original residues 248 to 255 of CCSIII, consisted of the sequence Ac-GLTIWEER-NH$_2$, where Ac– and –NH$_2$ correspond to the neutralizing acetyl- and amide- groups, respectively. Peptide 2 corresponds to the last seven residues at the C-terminus of CCSIII with a modified N-terminal alanine (Ac-AQPPAHL). Each peptide was titrated into a solution of 1 mM of PDZ2α, and the binding was followed by NMR. At each titration point, a 2D ^{1}H,^{15}N-HSQC spectrum of ^{15}N-labeled PDZ2α was recorded.
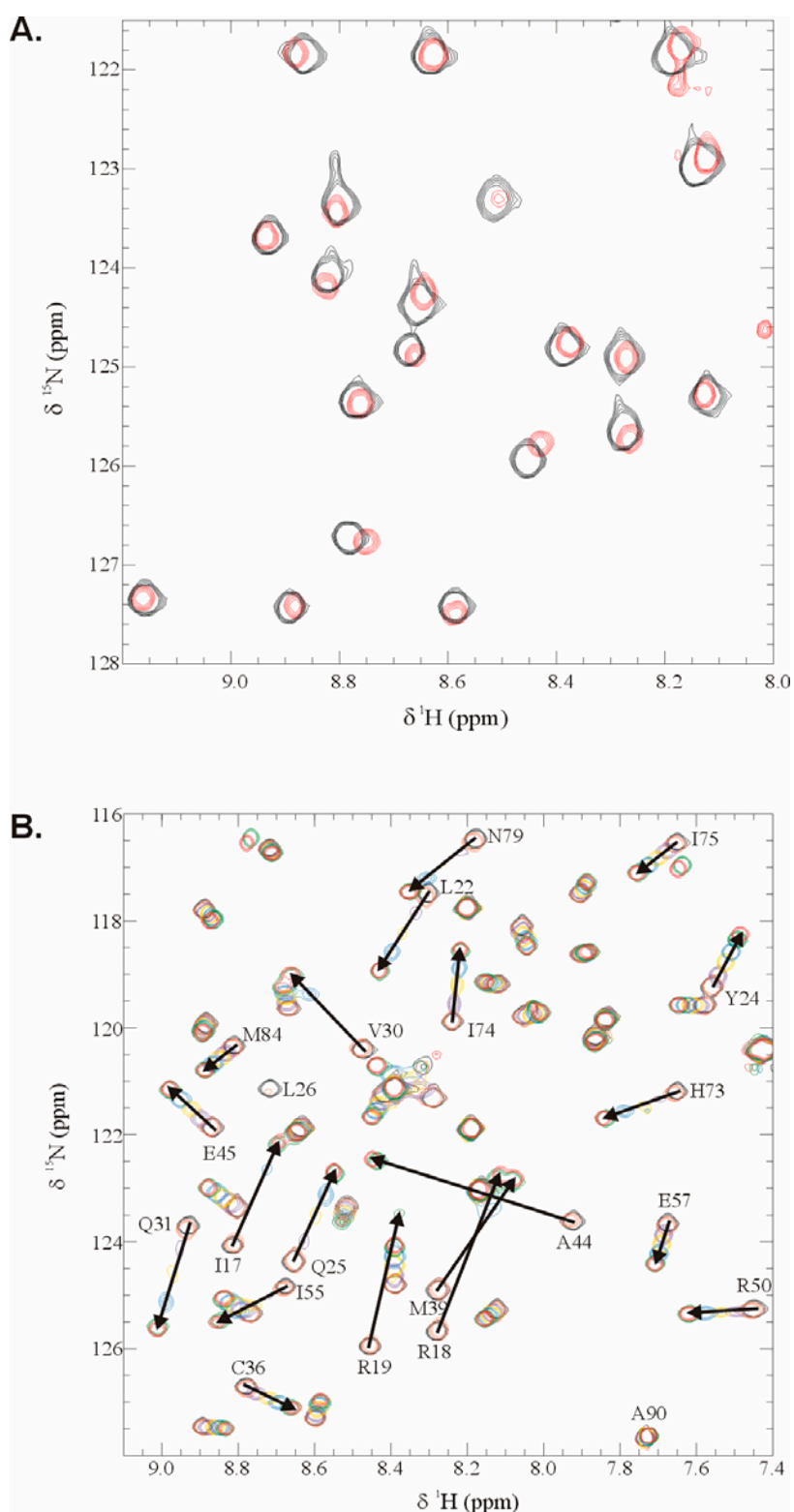
IV.3.1 - Ac-GLTIWEER-NH$_2$

Figure 4.1**A** shows the superposition of two spectra of PDZ2α. The black trace corresponds to the signal of the free domain, and the red trace corresponds to that of PDZ2α in the presence of 22.4 equivalents of Ac-GLTIWEER-NH$_2$. Each circle corresponds to the resonance of a backbone nitrogen and its proton. Addition of Ac-GLTIWEER-NH$_2$ to PDZ2α only resulted in very small chemical shift perturbations

in the HSQC spectrum at high peptide to protein ratio, from which it was concluded that no specific interaction occurred.
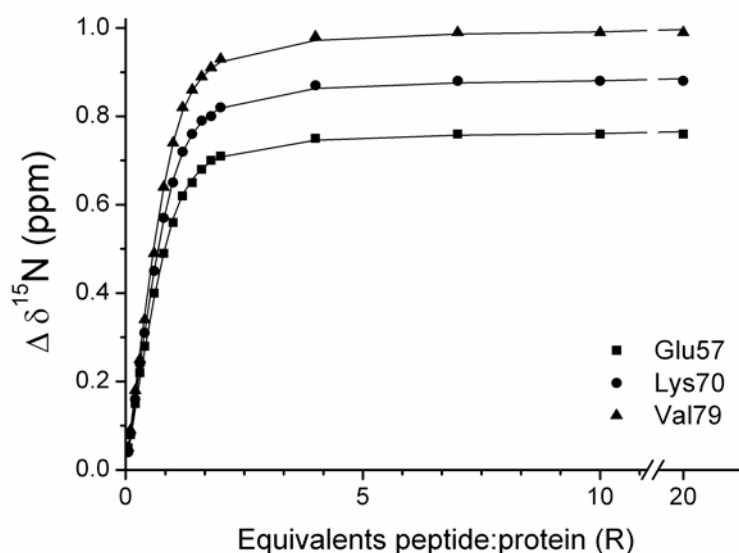
IV.3.2 - Ac-AQPPAHL

Ac-AQPPAHL corresponds to the C-terminal residues of CCSIII. The N-terminal group of this peptide is rendered neutral by converting it to an acetyl group ("Ac-"). The spectrum of the domain at each titration point (18 in total) was recorded by NMR. Figure 4.1**B** shows the overlay of 7 of these titration points. In contrast with the results obtained with the previous peptide, many resonances in the NMR spectrum PDZ2α exhibit a clear chemical shift perturbation upon addition of the Ac-AQPPAHL peptide, indicating a specific interaction between the peptide and the protein. Resonances with small perturbations remain visible during the entire titration, while others are broadened at the same peptide:protein ratio due to an intermediate exchange regime. At 20:1 peptide:protein ratio all resonances, with exception of Leu 26, reappear, indicating near-complete saturation of the protein with peptide.

Figure 4.1: **A.** Overlay of ¹H,¹⁵N-HSQC spectra of PDZ2α in the absence (black) and in the presence (red) of 22.4 equivalents of Ac-GLTIWEER-NH₂ to the protein; **B.** Chemical shift perturbation of PDZ2α upon addition of Ac-AQPPAHL. The overlaid spectra correspond to the following titration points: 0.0, 0.05, 0.3, 0.6, 1.0, 4.0, and 20.0 equivalents of peptide to protein. The direction of the perturbation is indicated by an arrow.

From the chemical shift perturbations, the dissociation constant (K_D) of PDZ2α for Ac-AQPPAHL was determined to be 91 ± 2 μM (see Figure 4.2).


Figure 4.2: Titration curves derived from the backbone nitrogen chemical shift perturbation of E57, K70, and V79 upon addition of Ac-AQPPAHL.

Figure 4.3**A** shows the maximum average shift ($\Delta\delta_{avg}$), averaged over the nitrogen and proton perturbation for all PDZ2α backbone amides, in the presence of 20 equivalents of Ac-AQPPAHL. The residues experiencing the largest perturbation have been grouped in two classes, according to the size of the perturbation. The three most affected residues are Gly 27 and Phe 28 of the canonical binding motif (as expected), and Ala 44. Four more residues are strongly affected by the binding of Ac-AQPPAHL: Arg 18, Asn 32, Ile 43 and Glu 69. As mentioned above, the extensive broadening of Leu 26 indicates that it must be among the most perturbed residues. However, the broadening precludes determination of the perturbation size.

All seven residues have been mapped onto the backbone of PDZ2α (see Figure 4.3**B**). The picture also shows the last four residues of the peptide (PAHL) modeled

in PDZ2α on the basis of the PSD-95-peptide complex (PDB accession code 1BE9 (Doyle *et al.*, 1996)). The model was obtained by structural alignment of PDZ2α and PAHL with the third PDZ domain of the synaptic protein PSD-95 bound to its peptide. The largest effects observed are corroborated by the presence of the last two residues of the peptide (His and Leu) in the close vicinity of Gly 27 and Phe 28. The effect observed on Ala 44 seems to be only indirect. Also for residues Arg 18 and Ile 43, it is unlikely that the peptide directly interacts with them. As for residues Asn 32 and Glu 69, they are situated at the bottom of the groove forming the binding pocket. The Pro seems to be close to residue Asn 32 of PDZ2α, both side chains stacking on top of each other. However, the distance between the proline side chain of the peptide and residue Glu 69 of PDZ2α is too large for direct interaction.
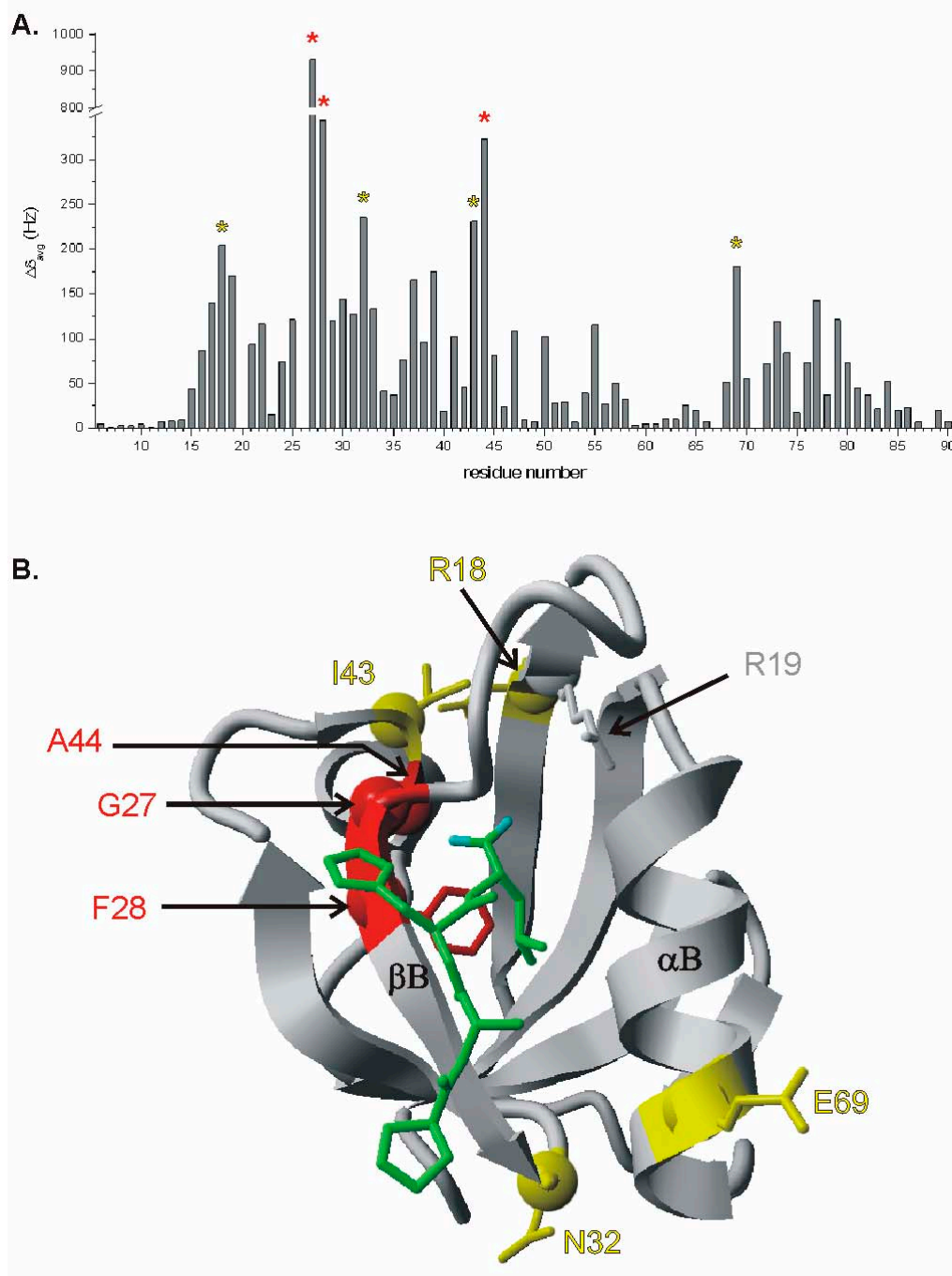
Figure 4.3: A. Histogram representation of the maximum average chemical shift perturbation ($\Delta\delta_{avg}$) in the presence of 20 equivalents of Ac-AQPPAHL. The residues of PDZ2α that experience a resonance shift larger than $\Delta\delta_{avg} > 250$ Hz upon addition of Ac-AQPPAHL are marked with a red asterisk. The residues that observe a resonance shift of 175 Hz $< \Delta\delta_{avg} < 250$ Hz bear a yellow asterisk; **B.** Mapping of the effect of Ac-AQPPAHL on PDZ2α. The color coding is the same as in A. The Cα atoms of relevant residues are represented by a sphere while the side chains are shown as sticks. The last four residues of peptide (PAHL) were modeled in PDZ2α on the basis of the PSD-95-peptide complex (PDB accession code 1BE9 (Doyle *et al.*, 1996)) and are represented in green. The atoms colored in cyan correspond to the C-terminal carboxylic group

It is observed that the shape of the signals changes during the titration of Ac-AQPPAHL into the PDZ2α solution. Figure 4.4 shows the decrease of intensity and broadening of the resonances of Gly 47 upon addition of Ac-AQPPAHL. After a ratio peptide:protein of 1:0.6, the signals sharpen up and regain intensity, typical of an increase in the free/bound exchange rate, and a change in the fractions away from 50%/50%. An analysis of these results indicates that the dissociation rate constant is on the order of 1000 s^{-1}. This results in a fast exchange regime for nuclei that exhibit small chemical shift perturbation and intermediate to slow exchange for the nuclei with large resonance frequency changes.
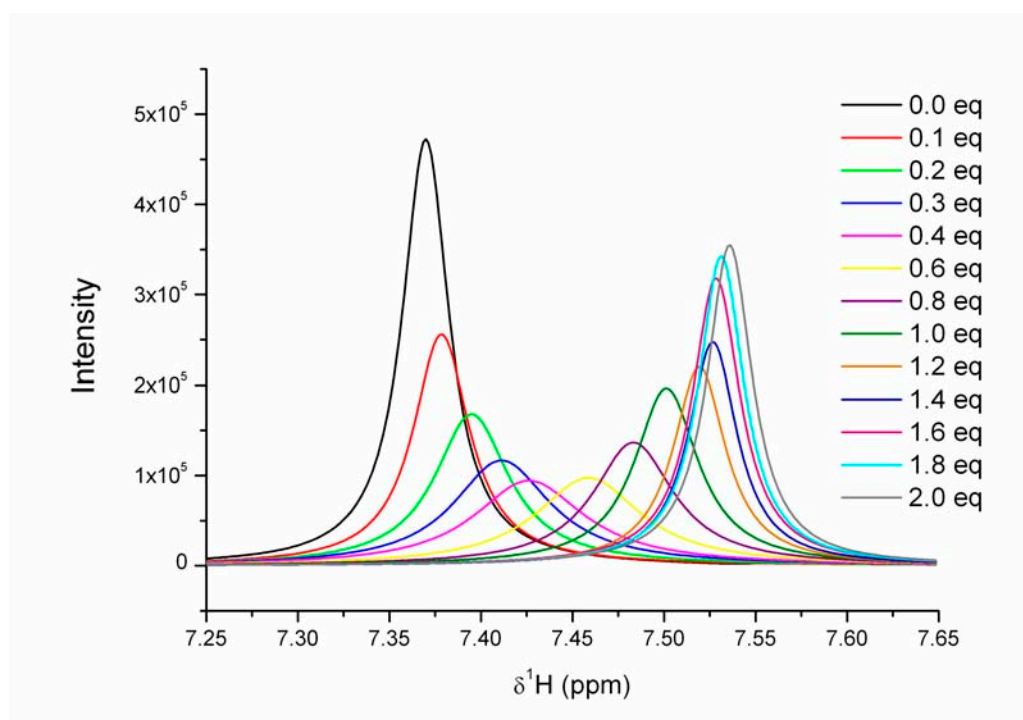

Figure 4.4: Cross-section through the ^{1}H resonance of Gly 47 of PDZ2α at different titration points with Ac-AQPPAHL. The ratios are indicated at the right hand side of the graph, in equivalents (eq) of Ac-AQPPAHL:PDZ2α.

IV.3.3 - Importance of the residues of Ac-AQPPAHL in binding

To establish the relative importance of the individual residues of the Ac-AQPPAHL peptide for binding to PDZ2α, titrations were performed with several peptide variants.

Interactions of PDZ domains with their C-terminal targets have been reported to involve the last four to six residues of the peptide (Fanning and Anderson, 1999), although interactions down to residue P_{-8} have also been postulated (Cai *et al.*, 2002; Birrane *et al.*, 2003). P_0 (denoting the C-terminal residue), P_{-1}, and P_{-3} residues were changed into an alanine, one at a time. Also, the influence of the N- and C-termini of the peptide on the affinity was studied. The binding affinities of PDZ2α for each peptide were derived from NMR titration experiments as described above. The respective dissociation constants are gathered in Table 4.1.

Table 4.1: Summary of the binding constants of PDZ2α for each studied peptide

peptide	K_D (± deviation) in μM
Ac-AQPPAHL	91 (± 2)
Ac-AQPPAHL**-NH₂**	$> 55 \cdot 10^3$
Ac-AQPPAH**A**	$14.3 (\pm 0.2) \cdot 10^3$
Ac-AQPPA**A**L	47 (± 4)
Ac-AQP**A**AHL	98 (± 2)
AQPPAHL	300 (± 8)

The largest changes in affinity are observed when the C-terminal residue (P_0) is altered. When the carboxyl-group is neutralized by converting it into an amide group, binding is completely abolished. When the P_0 residue is changed from a leucine to an alanine, the affinity decreases 160-fold. The presence of a positive charge at the P_{-6} residue of the peptide decreases the affinity by a factor 3. When the

proline P$_{-3}$ is changed into an alanine, the affinity remains unchanged. Interestingly, when the P$_{-1}$ histidine is changed into an alanine the affinity increases by a factor 2.

The titrations also reveal that a specific peptide variant affects specific residues of the PDZ2α domain. The absolute difference in chemical shift perturbation ($|\Delta_A|$) for each PDZ2α residue was quantified by subtracting its maximum average shift perturbation in the presence of the alanine variant to that of the native peptide (Ac-AQPPAHL). The residues of PDZ2α that show a different chemical shift perturbation pattern between the native peptide and the P$_0$ alanine-variant are the conserved Arg 19, Gly 27 and Phe 28 of the binding motif, residue Val 30, and residues His 73, Ile 74, Leu 75, Ser 76 and Asn 77 of the helix αB (annotated with red asterisks in Figure 4.5**A**). The only residue that is significantly affected by the P$_{-1}$-variant is Gly 27, although an effect on Leu 26 cannot be ruled out (annotated with a yellow asterisk in Figure 4.5**B**). Three residues, (Asn 32, Gly 33, and Glu 69, located towards the C-terminal side of βB and the N-terminal side of αB) sense the change at the P$_{-3}$ position (annotated with blue asterisk in Figure 4.5**C**).
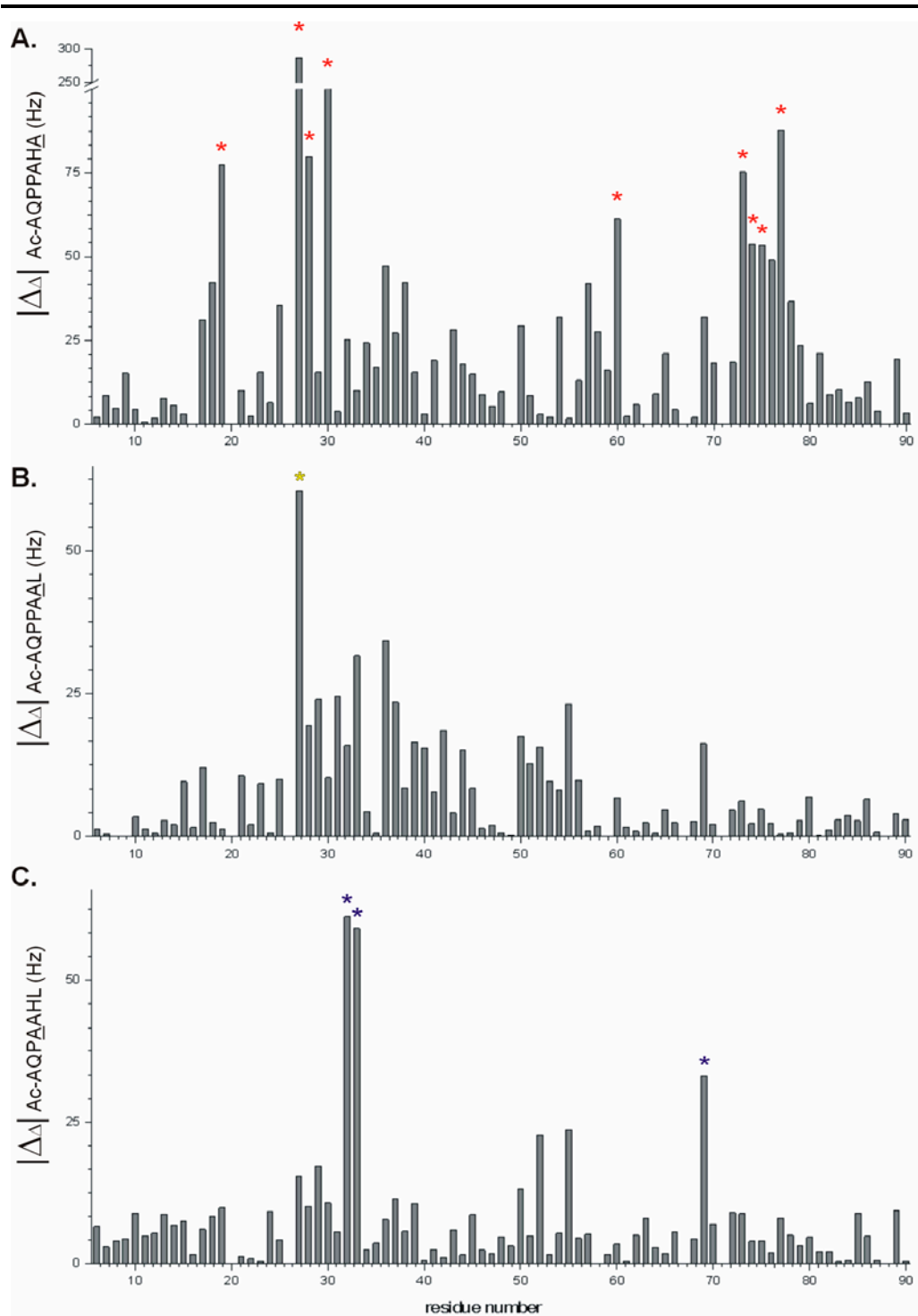
Figure 4.5: Histogram representation of the absolute difference of resonance shift ($|\Delta_\Delta|$) between the native peptide Ac-AQPPAHL and the alanine variants (the residue that is changed is underlined); **A.** $|\Delta_\Delta|$ with P_0 variant; **B.** $|\Delta_\Delta|$ with P_{-1} variant; **C.** $|\Delta_\Delta|$ with P_{-3} variant. The most affected residues are annotated with an asterisk.

The residues mentioned above have been mapped the structure of PDZ2α with the PAHL peptide modeled in (see Figure 4.6).
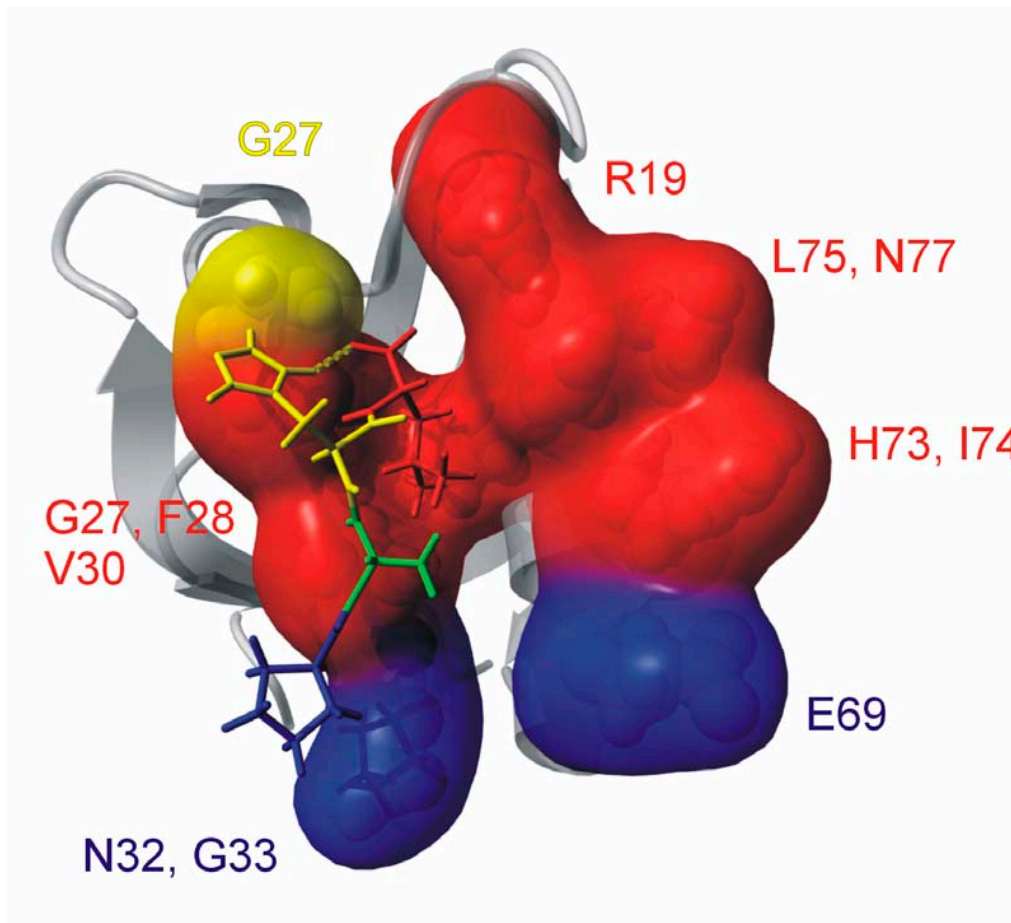
Figure 4.6: Model of the last four residues (PAHL) of CCSIII in the PDZ2α binding groove. The effects observed upon binding of the P_0, P_{-1} and P_{-3}-variants are represented in red, yellow and blue, respectively. The model was obtained by structural alignment of PDZ2α and PAHL with the third PDZ domain of the synaptic protein PSD-95 bound to its peptide ligand (PDB accession code 1BE9 (Doyle *et al.*, 1996)).

IV.4 - DISCUSSION

PDZ2α has an open peptide-binding groove capable of interaction with C-terminal ligands. Titration experiments showed clear evidence that PDZ2α specifically binds a peptide corresponding to the six C-terminal residues of CCS, with a 91 μM dissociation constant.

The loss of affinity resulting from the Leu to Ala mutation of the C-terminal residue or the chemical modification of the terminal carboxy-group clearly indicates that the peptide binds in a canonical fashion between βB strand and αB helix. We also examined the differential chemical shift effects upon changes of the CCSIII peptide. By quantifying these differences in chemical shift perturbation, it is possible to probe specific interactions between PDZ2α residues and residues in the peptide. Using the complex of PSD-95 and its ligand (PDB accession code 1BE9 (Doyle *et al.*, 1996)) as a template, we constructed a model of the PDZ2α–CCSIII peptide complex (see Figure 4.6).

Residues sensitive to the P_0 alanine-variant (see Figure 4.6, shown in red) line the top of the PDZ2α binding groove and illustrate its importance for binding. The side chain of the P_0 leucine is highly buried inside the binding groove, pointing towards the residues present in helix αB.

The P_{-1}-variant showed a surprising increase in affinity. The chemical shift analysis revealed that Gly 27 (in yellow in Figure 4.6) was the only residue significantly affected by this mutation. The imidazole ring of the histidine P_{-1} is oriented toward the Gly 27 residue of PDZ2α. The increased affinity observed for the P_{-1}-variant can be rationalized by the presence of a hydrogen bond between the imidazole ring of the P_{-1} histidine and the carboxy-terminal group of the peptide. When the P_{-1} histidine is changed into an alanine, this hydrogen bond can no longer be formed, and the carboxylic group becomes more available for binding to the protein. Residues at the P_{-1} position have traditionally been classified as unimportant for PDZ-target binding (Doyle *et al.*, 1996). However, more recent reports have illustrated their importance (Kang *et al.*, 2003a; Walma, 2004), suggesting that P_{-1} residues potentially provide an essential discriminatory role (Walma, 2004).

The P$_{-2}$ residue is traditionally a crucial determinant for either class I or class II peptides. It usually is a large hydrophobic residue pointing into the helix αB. But in the PDZ2α–CCSIII peptide complex, the P$_{-2}$ residue is an alanine. Its small hydrophobic side chain is well suited for an orientation inside the apolar interior of the protein, close to the side chain of Val 72. Finally, the P$_{-3}$ residue is located in the proximity of Asn 32 and Gly 33, at the C-terminus of βB, and Glu 69 at the N-terminus of αB, but it is not likely to be involved in binding as mutating it does not affect affinity.

CCSIII has been suggested to be a flexible domain, since it is not observed by X-ray diffraction methods in the crystals of CCS (Lamb *et al.*, 2001). This flexibility may well be an essential property of CCS in view of its function in copper transport (see Chapter 1). The crystal structure of the CCS–SOD1 shows that the CCS copper binding domain and that of SOD1 are too far apart for copper transfer. Instead, a mechanism in which transfer is mediated by CCSIII has been proposed (Falconi *et al.*, 1999; Rosenzweig and O'Halloran, 2000). Therefore, the inhibition of CCS activity observed by McLoughlin *et al.* (McLoughlin *et al.*, 2001) could be caused by restriction of the flexibility of CCSIII due to its interaction with PDZ2α. An alternative explanation might be that X11α localizes CCS away from its partners and thus prevents it to obtain or donate Cu.

Chapter V

Tag removal with Pd(II) compounds

ABSTRACT

A new generation of synthetic metalloproteases has recently been developed (by Prof. N. Kostic and collaborators at Iowa State University, USA) using transition metal complexes. These reagents present an alternative for existing proteases with several potential advantages: they are highly specific (for methionine and histidine side chains), they are capable of driving the reaction to completion and they leave the peptidic fragments devoid of any modifications. The efficiency of these compounds, on peptides as well as on whole proteins, has been well established at low pH and high temperature. At neutral pH and mild temperature, however, these compounds have worked on peptides only. The aim of the study presented here was to cleave a fusion protein using Pd compounds and to remove the tag moiety from the protein of interest. Their efficiency was tested here under mild conditions of pH and temperature. These preliminary studies did not show any cleavage activity of the tested Pd compounds under our conditions.

V.1 - INTRODUCTION

Technological advance and progress in research go hand in hand. For instance, protein purification can nowadays be done in a single step, with the use of specific affinity tags engineered on the protein of interest together with the use of high performance chromatography devices. Helpful as those tags may be during this purification process, they can turn out to interfere with the protein of interest at a later stage of the experimentation. To give an example, crystal growth requires extremely pure protein, for which the purification procedures are often time consuming, hence the use of a tag to speed up the process. But the widely used histidine-tag can be a hindrance for crystal growth. Another widely used tag (the GST-tag) has been shown to alter sometimes the properties of the protein to which it is fused, as in the case of the copper chaperone Cox17 (Srinivasan *et al.*, 1998; Heaton *et al.*, 2001).

Ongoing technical improvements may make the means available by which the tags can be removed after they have served their purposes. Usually, proteases are used after the purification step(s) in order to separate the tag from the protein of interest. Proteases present, however, a number of drawbacks. The first one concerns the specificity of their cutting sites. A particular protease usually only recognizes and cleaves a defined sequence of amino acids specific for that protease. This sequence is engineered between the protein of interest and the tag. However, the same sequence can also be present within the protein of interest resulting in undesired cleavage at this site. Secondly, the action of proteases is rarely brought to completion. After (long) incubation of the tagged protein with a protease, some of the chimerae still remain intact. Thirdly and most importantly, after tag removal, the protein of interest often bears some extra residues derived from the tag. The consequence of the first two drawbacks is the loss of precious material, time and money. The consequence of the third drawback is unwanted modifications on the protein of interest due to the presence of parts of the tag, even after cleavage.

Synthetic metalloproteases have emerged in the past few years as new reagents for protein analysis. Pd(II) compounds have been developed by Prof. N. Kostic and co-

workers (Iowa State University, USA) as a new generation of proteolytic reagents. These new compounds present several advantages. Firstly, they bind specifically to methionine side chains (later on called "the anchor") (Milovic and Kostic, 2001). Secondly, they drive the reaction to completion. And thirdly, they leave the protein of interest devoid of artificial residues. However these synthetic metalloproteases only work under extreme conditions of pH and temperature, unfavorable for biomacromolecules since they lose their properties. However, Milovic *et al.* have solved the problem by modifying the anchor of the Pd(II) compounds from a Met to a Pro–Met sequence (*vide infra*) (Milovic and Kostic, 2003).

The mechanism of action of Pd(II) has been studied in detail (see Scheme 5.1). The Pd(II) forms a stable six-membered chelate ring with the side chain sulphur of a methionine (the anchor) and the deprotonated amide nitrogen of the same methionine. In this way, the Pd(II) is properly positioned to promote cleavage of the second peptide bond N-terminal from the anchor (the X–Y bond in Scheme 5.1) (Milovic and Kostic, 2002). Two mechanisms of cleavage are possible as depicted in Scheme 5.1:

a) the Pd(II) compound coordinates the backbone oxygen of the second residue N-terminal from the anchor (O_x in Scheme 5.1), thereby further polarizing the $C=O_x$ bond and activating the first amide bond N-terminal from the anchor (the $C–N_y$ bond in Scheme 5.1) for nucleophilic attack by a solvent water molecule.

b) the Pd(II) compound activates one of its water ligands for nucleophilic attack of the X–Y peptide bond.

Polypeptide and protein cleavage with Pd(II) compounds has been demonstrated at pHs between 1.2 and 4.5, validating Pd(II) compounds as tools in analytical biochemistry (Zhu *et al.,* 1998; Qiao *et al.,* 1999). At higher pH however, the protease activity is inhibited because of the formation of stable tri-and tetra-dentate complexes between the Pd(II) compounds and the peptide (or protein) (see Scheme 5.2 **1a**-**4a**).
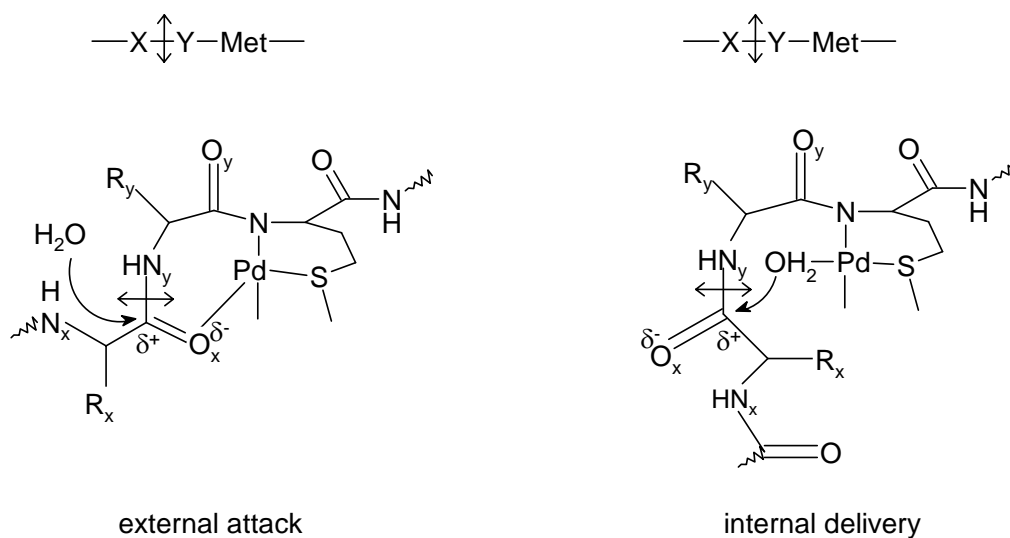
Scheme 5.1: Two mechanisms of Pd(II) mediated peptide bond cleavage

As mentioned earlier, the low pHs used do not allow to maintain the native properties of many protein of interest. However, Milovic and Kostic have shown in more recent studies that the activity inhibition at higher pH can be overcome when the anchoring methionine is preceded by a proline, leading to improved specificity of cleavage and the possibility to work at neutral pH (Milovic and Kostic, 2003). The mechanism by which this is possible is shown in Scheme 5.2. After formation of the active bidentate complex between the protein and the Pd(II) (complexes **2a** and **2b** in Scheme 5.2), the first and the second backbone nitrogen N-terminal from the anchor can be deprotonated by the Pd(II) and form the inactive tri- and tetra-dentate complex **3a** and **4a**. The pKa of this reaction is lower than 2.3, although the proteolytic activity of the Pd(II) is not inhibited until pH 4.5 is reached. Thus, if the backbone nitrogen of the residue preceding the anchor does not carry any hydrogen, as in the case of tertiary amides, the complex **3a** (and thus **4a**) cannot be formed. Such requirements are met by prolines. By using a Pro–Met sequence, the authors succeeded in cleaving 14-mer peptides with Pd(II) compounds at pHs as high as 7.0. The average occurrence of prolines and methionines is low (5.2% and 2.2% respectively) (Doolittle, 1989). Thus a Pro–Met sequence has a low occurrence in natural proteins. It is thus an interesting target sequence to split chimera proteins

that are obtained through fusion of a protein and a tag, for instance. Such a chimera should possess a Pro-Met sequence engineered between the C-terminus of the protein of interest and the N-terminus of the tag. For this application, a mild pH and temperature of incubation with Pd(II) can be used and the integrity of the protein of interest can be preserved.

The PDZ2α domain that has been subjected to study in the previous chapters is very stable and well characterized. It is thus a good test-protein to examine the feasibility of Pd(II)-mediated tag removal under neutral pH and mild temperature conditions. For this purpose, a chimera was especially constructed with the free PDZ2α domain, an engineered Pro–Met sequence and a six-histidine-GST tag.
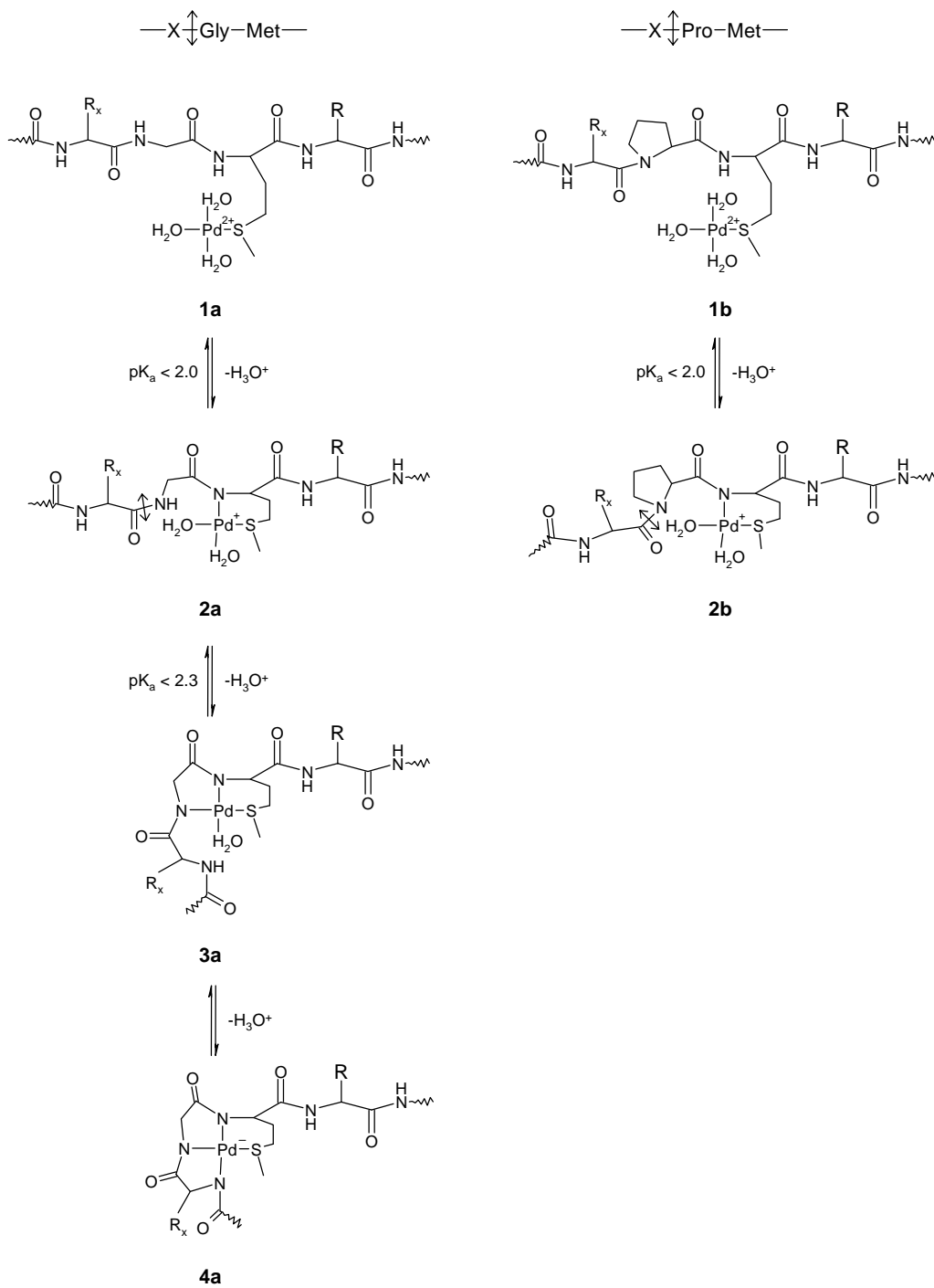
Scheme 5.2: Difference of binding between and X–Gly–Met and a X–Pro–Met

V.2 - MATERIALS AND METHODS

V.2.1 - Cloning of the chimera protein

A plasmid containing the PDZ2α-PM-His₆-GST was constructed in two steps. First, a plasmid coding for the His6-GST tag (pET-tag) was constructed. The GST gene was amplified by PCR from the plasmid pRP265Nb (de Jong *et al.*, 2002) with the following two primers: `5'-TCACCTCGAGATGTCCCCTATACTAGGTTATTGGAAAA-TTAAGGG-3'` (coding strand) and `5'-TACAGATCTTATTTTGGAGGATGGTCGCC-3'` (non-coding strand). The amplified fragment was digested with XhoI/BglII, and inserted into the XhoI/BamHI sites of a pET3H plasmid (Chen and Hai, 1994).

A plasmid containing the sequence coding for PDZ2α (residues 745 to 823 of X11α plus engineered Gly and Asn residues at the N-terminus) was already available in the lab and was used as a template. The PDZ2α sequence was amplified by PCR using the following set of primers: `5'-GCGAAATTAATACGA-CTCACTATAGGG-3'` (coding strand) and `5'-GTGATGCATTGGCGCGGCTGGCA-TTG-3'` (non-coding strand). The amplified fragment was digested with XbaI/NsiI and inserted into the XbaI/NsiI sites of the pET-tag plasmid mentioned above, resulting in the final plasmid pET-PDZ-PM-His₆-GST.

V.2.2 - Expression and purification

A preculture was prepared in 1.5 ml of rich medium containing 100 μg/ml ampicillin, 25 μg/ml chloramphenicol, 1% glucose and inoculated with 1 μl of a -80°C glycerol stock of *E.coli* BL21 (DE3*RP transformed with the plasmid pET-PDZ-PM-His₆-GST) and grown overnight at 28°C. This preculture was used to inoculate 150 ml of fresh rich medium (prepared as mentioned above). Over-expression was induced by addition of 0.5 mM IPTG at OD_{600} = 0.7 and the incubation was continued for 3 hours. The cells were then collected by centrifugation, resuspended in 2 ml MilliQ water, and kept at -80°C until the next step. After thawing, the cells were sonicated in the presence of 1 mM PMSF and 0.1% NP-40 (a non-ionic detergent). Sodium phosphate and NaCl were added to the lysate to 10 mM pH 8.0

and 250 mM respectively, followed by centrifugation at 13,000 g for 30 minutes. The supernatant was loaded onto a Ni-NTA resin (Qiagen) saturated with nickel and eluted with a step gradient of imidazole (5, 50, and 200 mM in 10 mM sodium phosphate buffer pH 8.0 250 mM NaCl). The eluted fractions were analyzed on 15% Tris/Tricine/SDS PAGE. Those exhibiting a single band below 40 kDa on the gel were pooled and dialyzed extensively against MilliQ water. Precipitates were removed by centrifugation for 10 minutes at 16,000 g. The protein concentration was determined by UV-spectroscopy at 280 nm (ε = 45 mM^{-1} cm^{-1} was estimated using the ProtParam software (available at http://us.expasy.org/tools/protparam.html).

V.2.3 - Palladium compounds

The following two compounds were used:

Pd(en): cis-[Pd(en)(H$_2$O)$_2$](ClO$_4$)$_2$; [Pd(H$_2$O)$_4$]: [Pd(H$_2$O)$_4$](ClO$_4$)$_2$, which were generously provided by Prof. Kostic from Iowa State University. A schematic representation of the two compounds is shown in Scheme 5.3.
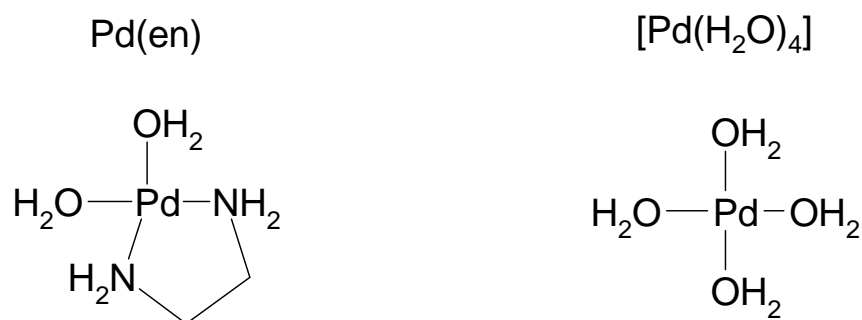
Scheme 5.3: Drawing of the two palladium compounds used in this study

V.2.4 - Experimental conditions to test the tag cleavage

Two buffers were used: MES pH 6.0 or HEPES pH 7.0

Non denaturing conditions: vials containing 0.1 M of either buffer, 11 μM chimera, 100 μM Pd(en) or [Pd(H$_2$O)$_4$] in a final volume of 100 μl were incubated for 24 hours at 4°C, room temperature (RT), or 37°C. Concentrated NaOH was added to correct the pH if needed.

Denaturing conditions: vials containing 5.4 M urea in either buffer, 11 μM chimera, 100 μM Pd(en) or [Pd(H$_2$O)$_4$] in a final volume of 100 μl, were incubated 24 hours at RT, 37°C, or 60°C. Control experiments were performed in the same buffer and under the same reaction conditions but without Pd(II).

V.3 - RESULTS

A chimera protein was constructed, consisting of the second PDZ domain of the neuronal adaptor X11α (PDZ2α), a tag made of a Pro-Met sequence followed by six histidines and a GST (see Figure 5.1).


```
MGNVTTVLIR  RPDLRYQLGF  SVQNGIICSL  MRGGIAERGG  VRVGHRIIEI
NGQSVVATPH  EKIVHILSNA  VGEIHMKTMP  AAPMHHHHHH  LEMSPILGYW
KIKGLVQPTR  LLLEYLEEKY  EEHLYERDEG  DKWRNKKFEL  GLEFPNLPYY
IDGDVKLTQS  MAIIRYIADK  HNMLGGCPKE  RAEISMLEGA  VLDIRYGVSR
IAYSKDFETL  KVDFLSKLPE  MLKMFEDRLC  HKTYLNGDHV  THPDFMLYDA
LDVVLYMDPM  CLDAFPKLVC  FKKRIEAIPQ  IDKYLKSSKY  IAWPLQGWQA
TFGGGDHPPK
```

Figure 5.1: Primary structure of the chimera. The sequence of PDZ2α is written in normal font, the histidine moiety of the-tag is underlined, while its GST component is written in italics. The Pro–Met sequence is presented in bold, between the PDZ2α domain and the tags.

The removal of the tag from PDZ2α was attempted by means of incubation of the chimera at neutral pH (6 or 7), at temperatures ranging from 4°C up to 60°C, under native or denaturing conditions, and in the presence of one of the two Pd(II) compounds (Pd(en) or [Pd(H$_2$O)$_4$]).

The palladium compounds were expected to bind the Pro-Met sequence at the methionine, with cleavage occurring at the peptide bond N-terminal from the proline releasing the intact PDZ2α from the Pro-Met-His$_6$-GST moiety of the chimera. In case of cleavage, the band of the chimera is expected to disappear from the SDS-PA gel, and two bands corresponding to PDZ2α and the tag should appear at 8 and 27 kDa, respectively.

V.3.1 - Non denaturing conditions

The cleavage of the tag was tested for both Pd(II) compounds in MES buffer pH 6 and HEPES buffer pH 7. After 24 hours of incubation at 4°C, RT, or 37°C, each sample was loaded on a 15% Tris-glycine SDS-PA gel (see Figure 5.2).
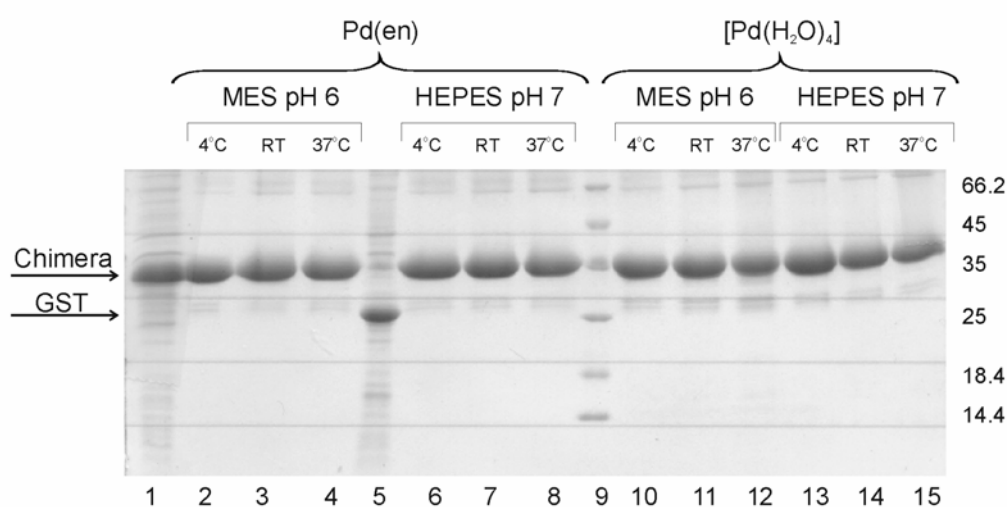
Figure 5.2: Effect of the Pd(II) compounds on the chimera protein. (1) & (5) whole cells expressing the chimera protein and GST alone respectively; (9) standard molecular mass marker (the masses are indicated at the right hand side of the gel in kDa).

Lanes 1 and 5 show the bands of the intact chimera and of the GST alone, respectively. None of the non-denaturing conditions tested here yield bands at the expected positions (8 and 27 kDa). This indicates that cleavage did not occur. It is conceivable that the arrangement of PDZ2α and GST with respect to each other

buries the cleavage site, making it unavailable to the Pd(II) compounds. Therefore, similar experiments were performed under denaturing conditions.

V.3.2 - Denaturing conditions

The same Pd(II) compounds as mentioned above were used in this series of experiments. The denaturing agents are 5.4 M urea (in MES pH 6 or HEPES pH 7) and high temperature. After 24 hours of incubation (with and without Pd(II) compounds) at RT, 37°C or 60°C, the samples were loaded on a 15% Tris-glycine SDS-PA gel (see Figure 5.3**A** and 5.3**B**). Figure 5.3 shows that the presence of urea does not promote the cleavage. None of the bands is replaced by two smaller ones at the expected sizes. However, lanes A4 and A6 do present a difference when compared to their controls shown in lanes A3 and A5. The major band is less intense, indicating that some protein has been lost, and appears to run at a slightly higher position on the gels. If the Pd(II) present in these experiments is responsible for that loss, no specific degradation is yet observed. Similar observations are made in lanes A11, A12, B6, B7, B13, and B14 with a less intense band, also indicating loss of material, and at a slightly higher position. However, given that A11, B6 and B13 do not contain any Pd(II) compound, the shift in the band position cannot be attributed to the Pd(II) compounds. The reason for this small shift is unclear.
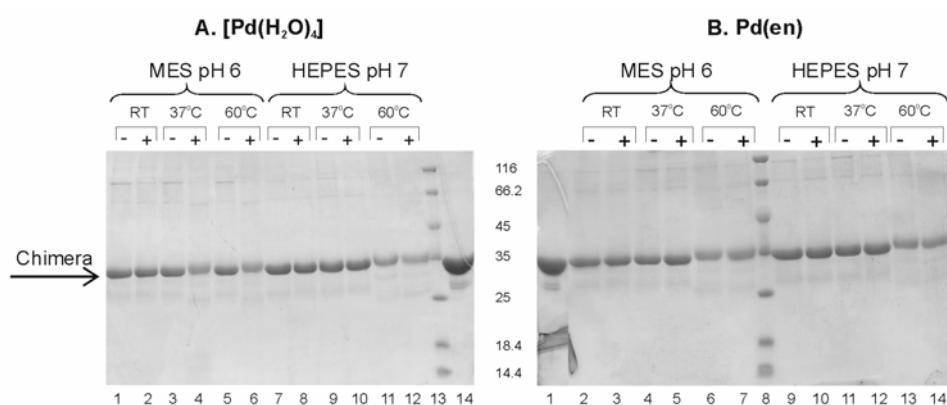
Figure 5.3: Effect of Pd(II) compounds on the chimera under denaturing conditions; **A.** Experiments done with 9 equivalents [Pd(H$_2$O)$_4$] to the chimera; (13) standard molecular mass marker; (14) purified chimera; **B.** Experiments done with 10 equivalents Pd(en) to the chimera. (1) purified chimera; (8) standard molecular mass marker. The molecular masses are indicated between the two gels in kDa; (-) & (+) indicate the absence and the presence of Pd(II) compound.

V.4 - DISCUSSION

Pd(II) has been shown in the literature to work well as a specific protease in acidic solutions. The low pH used by Milovic *et al.* however is often not suitable for proteins to maintain their native conformation. In order to preserve their integrity, neutral pH and mild temperature conditions are necessary. Theoretically, Pd(II) compounds should be able to interact and cleave specifically at the sequence Pro–Met. However, the protease activity of Pd(II) compounds under the mild conditions that have been tested here, could not be observed. Several factors may explain the absence of any digestion.

Firstly, there are 12 methionines in the chimera that may compete with the targeted methionine of the Pro–Met sequence.

Secondly, Pd(II) can also bind histidines (Milovic and Kostic, 2001). Although the current pH conditions are too high for cleavage from histidyl anchors, the 16 histidine residues present in the chimera may be possible competitors of the Pro–Met sequence for binding the Pd(II) compounds.

From the X-ray structure of the GST (PDB accession code 1GNE) (Lim *et al.*, 1994) and the NMR structure of PDZ2α (PDB accession code 1Y7N) (see Chapter 3), only 5 out of the 28 Met/His side chains are buried inside the GST, leaving a total of 23 potential competitors of the targeted Pro–Met sequence. It appears thus that the applied 10:1 ratio of Pd(II) to the chimera may be insufficient. Possibly, the removal of the His-tag (at the DNA level) or its saturation with another metal, or the use of a different tag can shed further light on this problem.

Thirdly, is that Pd(II) compounds are also known to bind and react with urea (Kaminskaia and Kostic, 1998). However, this reaction has only been reported in alcohol and/or acetone. Therefore any interference from urea under the conditions used is not expected.

Finally, our experiments were done in the presence of buffers, while the studies of Milovic *et al.* were done in pure aqueous solutions. The buffers that were used are so called Good's buffers. They are supposed not to react with metal ion, but they may still interfere with the Pd(II) compounds. The same experiments as those presented

here should thus be conducted in the absence of the buffers, with all the precautions regarding the pH of the reaction mixture containing the chimera to be taken into account.

The binding of the Pd(II) compounds on the chimera has also been assumed, but it has not been confirmed. HPLC experiments may shed light on the presence of the possible species of chimera present in the reaction mixture (without Pd(II) and with 1 or several Pd(II) bound), followed by MALDI-TOF analysis on the different fractions to determine the Pd(II) content of each fraction.

Further experiments in this direction are planned.

Chapter VI

Summary

&

General discussion

The goals of the research presented in this thesis were to solve the structure of the PDZ2α domain and to determine the interaction mode with CCSIII. A summary of the results is presented below followed by some concluding remarks.

VI.1 - STRUCTURE OF PDZ2α

The near-complete assignment of the resonances of PDZ2α (**Chapter II**) allowed to proceed with the calculation of the structure of PDZ2α (**Chapter III**). The resulting ensemble of 20 superimposed models shows a well-defined structure. The sequence conservation among different PDZ domains is rather low (see Figure 3.2**A**). However, the PDZ fold is conserved in PDZ2α, with six β-strands and two α-helices which superimpose well onto known PDZ domains, although the CSI prediction performed on the basis of the chemical shifts given in Chapter 2 had indicated only 4 β-strands (see Figure 6.1). All actual secondary structure elements are longer than predicted on the basis of the CSI.
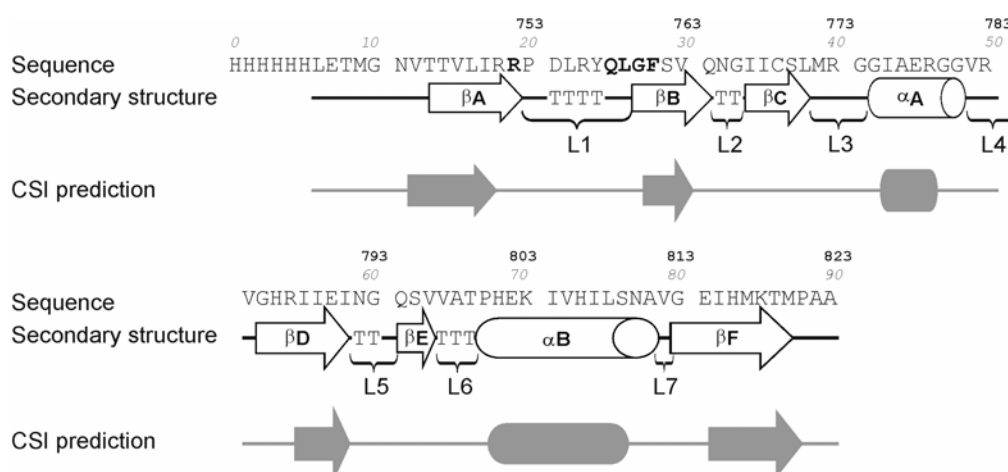
Figure 6.1: Comparison of the secondary structure of PDZ2α described in Chapter 3 with the CSI prediction obtained from the chemical shift assignments in Chapter 2.

The structural alignment with the third PDZ domain of Psd-95 (PDB code 1BE9 (Doyle *et al.*, 1996)) and the second PDZ domain of PTP-BL (PDB code 1GM1 (Walma *et al.*, 2002) revealed two special features of PDZ2α (see Figures 3.2**B**), *i.e.* the two loops flanking the βB strand (that holds the consensus binding motif) are

longer and shorter, respectively, than in other reported PDZ structures. However, the conserved residues involved in complex formation are maintained in their positions for ligand binding.

VI.2 - INTERACTION WITH PEPTIDES OF **CCSIII**

Probing of the two candidate sequences of CCSIII allowed us to attribute the interaction with PDZ2α to the last four residues of CCSIII (PAHL) and not to the internal sequence (**Chapter IV**).

The dissociation constant (K_D) of PDZ2α for Ac-AQPPAHL was determined to be 91 ± 2 μM. This value is in the range of other NMR determined dissociation constants of PDZ-ligand complexes, with values in the low μM to several hundreds μM range (Harris *et al.*, 2001; van den Berk *et al.*, 2004). It was concluded that PDZ2α and Ac-AQPPAHL are in a fast exchange regime, with a k_{off} in the order of 1000 s^{-1}.

It is interesting to compare the observed chemical shift perturbations of this study with those of other protein complexes. Recently, it has been suggested (Worrall *et al.*, 2001; Worrall *et al.*, 2002) that the perturbation size is an indication of the nature of the complex. In highly dynamic complexes, in which the partners do not assume a single well-defined orientation, the observed perturbations are very small and involve mainly charged residues. Complexes with more defined interactions show larger perturbations upon formation of the complex. Compared to other complexes with such high off-rates, the perturbations observed here are quite large (see Table 6.1), in agreement with a highly specific interaction. It is believed that in particular changes in the water structure on the protein surface, due to burial of surface residues in the interface causes chemical shift changes of amide nuclei. Thus, hydrophobic and polar, uncharged residues usually exhibit the larger changes in well-defined complexes.

Table 6.1: Comparison of the characteristics of four transient complexes: cytochrome *c* – plastocyanin (cyt *c* – Pc) (Ubbink and Bendall, 1997), cytochrome *c* – cytochrome *c* peroxidase (cyt *c* – CcP) (Worrall *et al.*, 2001), cytochrome *c* – myoglobin (cyt *c* – Mb) (Worrall *et al.*, 2002), PDZ2α – CCSIII (Chapter 4).

	Type of complex	Size of $\Delta\delta_{avg}$	Affected residues	Binding
cyt *c* – Pc (Ubbink and Bendall, 1997)	dynamic ensemble of orientations	up to 0.02 ppm	mostly acidic	10 μM
cyt b_5 – Mb (Worrall *et al.*, 2002)	dynamic ensemble of orientations	up to 0.02 ppm	acidic	20 μM
cyt *c* – CcP (Worrall *et al.*, 2001)	largely single orientation	up to 0.3 ppm	hydrophobic, uncharged polar	5 μM
PDZ2α – CCSIII (Chapter 4)	single orientation	up to 1.2 ppm	hydrophobic	100 μM

The study of the alanine variants of the CCSIII C-terminal peptide led to a further characterization of the interaction, and the results are summarized in Table 6.2, highlighting here the change in affinity (compared with Table 4.1).

Table 6.2: Summary of the binding constants of PDZ2α for each studied peptide

peptide	K_D (μM)	**Change in affinity**
Ac-AQPPAHL	91	-
Ac-AQPPA**A**L	47	↑ **2x**
Ac-AQP**A**AHL	98	**no change**
AQPPAHL	300	↓ **3.3x**
Ac-AQPPAH**A**	14,300	↓ **160x**
Ac-AQPPAHL-**NH₂**	> 55,000	↓ **> 600x**
Ac-GLTIWEER-NH₂	nd	-

These results confirm a canonical mode of interaction between PDZ2α and CCS. Indeed, the greatest determinant for complex formation is the free carboxyl-terminal group. The results of the alanine variants study suggest that only the last 3 residues of CCSIII interact directly with PDZ2α, as the P-3 variant does not affect the binding constant.

It was observed that the P_{-1} variant affects only one residue on PDZ2α (Gly 27) when compared to the "native" peptide. The residues of PDZ2α that are affected by the P_{-3} variant are Asn 32, Gly 33, and Glu 69. It is noteworthy that Gly 27 is situated at the N-terminal side of the βB-strand, and that Asn 32, Gly 33, and Glu 69 are at the C-terminal end of βB and N-terminal end of αB. Besides, the modeling of the residues PAHL into PDZ2α suggests that P_{-1} is rather surface exposed.

In view of these results, the CCSIII C-terminal peptide can be classified as a P2 type of PDZ ligand, according to the criteria defined by Walma (Walma, 2004).

The sequence alignment of the PDZ2 domain of X11α, β and γ (named PDZ2α, β and γ, respectively) is shown in Figure 6.2. The colored residues correspond to that of Figure 4.5: the residues of PDZ2α affected most by the P_0 alanine-variant are highlighted in red, those affected by the P_{-1} variant are highlighted in yellow, and those affected by the P_{-3} variant are highlighted in blue. The alignment shows that four residues out of the 11 colored in the picture are of a different nature in PDZ2β and γ compared to PDZ2α (position 32, 69, 73 and 77). The residue at position 74 differs between the three PDZ domains, but it is always a hydrophobic one. As observed in the PDZ2α structure (see Figure 4.6), the side chains of residues Asn 32, Glu 69, His 73 and Asn 77 are surface exposed, thus unlikely to interact directly with the peptide. Therefore, it can be hypothesized that the nature of these residue is not essential, as long as the backbone is available for interaction. Therefore, we can speculate that the C-terminal end of CCS binds to the second PDZ domain of all X11 family members, enhancing the possible role of X11 protein in copper homeostasis.
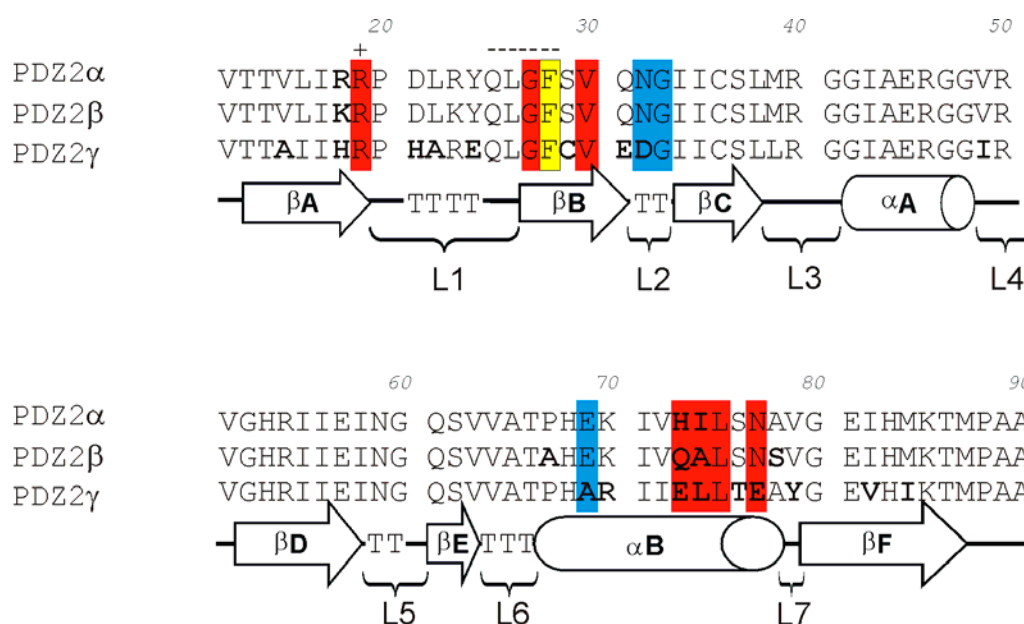
Figure 6.2: Sequence alignment of the second PDZ domain of X11α, X11β and X11γ (PDZ2α, PDZ2β and PDZ2γ, respectively). The residues that differ between the three PDZ2 domains are indicated in bold. The conserved arginine (R19) coordinating the ligand via a water molecule in other PDZ-peptide complexes is indicated with a '+', and the conserved binding motif (Q25 to F28) is indicated with '---'. The residues of PDZ2α (and their homologues in PDZ2β and PDZ2γ) interacting with the P_0 residue of the CCSIII peptide are highlighted in red. The one interacting with P_{-1} is highlighted in yellow. Those interacting with P_{-3} are highlighted in blue.

As argued in Chapter 1, the flexibility of CCSIII may be essential for copper loading of SOD1 by the chaperone (Lamb *et al.*, 2001). The crystal structure of the yeast CCS–SOD1 complex shows that the copper binding domains of CCS (the N-terminal ATX1-like domain) and SOD1 are too far apart for direct copper transfer. Alternatively, the transfer is proposed to be mediated via CCSIII, as it possesses a potential copper binding motif (Cys–X–Cys) (Falconi *et al.*, 1999; Rosenzweig and O'Halloran, 2000).

The interaction between CCSIII and PDZ2α, characterized in Chapter 4, and the consequent inhibition of CCS activity observed by McLoughlin *et al.* (McLoughlin *et al.*, 2001) could be caused by restriction of the flexibility of CCSIII upon interaction with PDZ2α. An alternative explanation might be that, upon binding, X11α physically keeps CCS away from its partners, thus preventing it from obtaining and/or donating Cu.

VI.3 - ENZYMATIC PROPERTIES OF PALLADIUM

   ## COMPOUNDS

Biotechnological research keeps providing scientists with easier, faster and more specific techniques. Prof. N. Kostic (Iowa State University, USA) has developed a series of Pd compounds with protease activities. Under denaturing conditions (low pH and high temperature) Pd compounds are able to bind histidine and methionine side chains, and cleave peptides N-terminal from those residues. There are numerous examples of Pd-mediated cleavage of peptides or proteins in literature (Zhu *et al.*, 1998; Qiao *et al.*, 1999; Milovic and Kostic, 2002). One of the aims is to use them as specific reagents for tag removal of fusion proteins. It was found that a Pro-Met sequence allows Pd compounds to cleave peptides N-terminal from the proline at pH as high as 7 (Milovic and Kostic, 2003). The Pd compounds are thus candidates for removal protocols, as these mild reaction conditions should not alter the biochemical/physical properties of the protein of interest. The work presented in **Chapter V** was aimed at confirming the feasibility of Pd-mediated tag removal under mild conditions. A chimera protein consisting of the PDZ2α domain (studied in chapter 2, 3 and 4) followed by the Pro-Met sequence and a His$_6$-GST tag was used to test the proteolytic properties of two Pd-compounds (Pd(en) and [Pd(H$_2$O)$_2$]) at pH 6 and 7. No protease activity of the tested Pd compounds could be observed under our conditions. The histidines and methionines represent almost 10% of the total number of residues in the chimera. Although they should not react, they might still compete for binding the Pd compounds.

This study is the first of a series of experiments that may lead to the introduction of Pd compounds as a tool for tag-removal under non-denaturing conditions for the protein of interest.

Reference list

Bezprozvanny, I. and Maximov, A. (2001), Classification of PDZ domains, *FEBS Lett.* **509**, 457-462.

Biederer, T., Cao, X.W., Sudhof, T.C., and Liu, X.R. (2002), Regulation of APP-dependent transcription complexes by Mint/X11s: Differential functions of mint isoforms, *J. Neurosci.* **22**, 7340-7351.

Biederer, T. and Sudhof, T.C. (2000), Mints as adaptors - Direct binding to neurexins and recruitment of Munc18, *J. Biol. Chem.* **275**, 39803-39806.

Birrane, G., Chung, J., and Ladias, J.A.A. (2003), Novel mode of ligand recognition by the Erbin PDZ domain, *J. Biol. Chem.* **278**, 1399-1402.

Brünger, A. (1992), X-PLOR, version 3.1. A system for X-ray crystallography and NMR,

Butz, S., Okamoto, M., and Sudhof, T.C. (1998), A tripartite protein complex with the potential to couple synaptic vesicle exocytosis to cell adhesion in brain, *Cell* **94**, 773-782.

Cai, C., Coleman, S.K., Niemi, K., and Keinanen, K. (2002), Selective binding of synapse-associated protein 97 to GluR-A alpha-amino-5-hydroxy-3-methyl-4-isoxazole propionate receptor subunit is determined by a novel sequence motif, *J. Biol. Chem.* **277**, 31484-31490.

Chen, B.P.C. and Hai, T.W. (1994), Expression Vectors for Affinity Purification and Radiolabeling of Proteins Using Escherichia-Coli as Host, *Gene* **139**, 73-75.

Cornilescu, G., Delaglio, F., and Bax, A. (1999), Protein backbone angle restraints from searching a database for chemical shift and sequence homology, *J. Biomol. NMR* **13**, 289-302.

Culotta, V.C., Klomp, L.W.J., Strain, J., Casareno, R.L.B., Krems, B., and Gitlin, J.D. (1997), The copper chaperone for superoxide dismutase, *J. Biol. Chem.* **272**, 23469-23472.

Dancis, A. (1998), Genetic analysis of iron uptake in the yeast Saccharomyces cerevisiae, *J. Pediatr.* **132**, S24-S29.

Dancis, A., Yuan, D.S., Haile, D., Askwith, C., Eide, D., Moehle, C., Kaplan, J., and Klausner, R.D. (1994), Molecular Characterization of a Copper Transport Protein in Saccharomyces-Cerevisiae - an Unexpected Role for Copper in Iron Transport, *Cell* **76**, 393-402.

de Jong, R.N., Mysiak, M.E., Meijer, L.A.T., van der Linden, M., and van der Vliet, P.C. (2002), Recruitment of the priming protein pTP and DNA binding occur by overlapping Oct-1 POU homeodomain surfaces, *Embo J.* **21**, 725-735.

Delaglio, F., Grzesiek, S., Vuister, G.W., Zhu, G., Pfeifer, J., and Bax, A. (1995), Nmrpipe - a Multidimensional Spectral Processing System Based on Unix Pipes, *J. Biomol. NMR* **6**, 277-293.

Doolittle, R.F. (1989), Prediction of protein structure and the principle of protein conformation,

Doyle, D.A., Lee, A., Lewis, J., Kim, E., Sheng, M., and MacKinnon, R. (1996), Crystal structures of a complexed and peptide-free membrane protein-binding domain: Molecular basis of peptide recognition by PDZ, *Cell* **85**, 1067-1076.

Falconi, M., Iovino, M., and Desideri, A. (1999), A model for the incorporation of metal from the copper chaperone CCS into Cu,Zn superoxide dismutase, *Structure* **7**, 903-908.

Fanning, A.S. and Anderson, J.M. (1999), PDZ domains: fundamental building blocks in the organization of protein complexes at the plasma membrane, *J. Clin. Invest.* **103**, 767-772.

Feng, W., Fan, J.S., Jiang, M., Shi, Y.W., and Zhang, M. (2002), PDZ7 of glutamate receptor interacting protein binds to its target via a novel hydrophobic surface area, *J. Biol. Chem.* **277**, 41140-41146.

Feng, W., Shi, Y.W., Li, M., and Zhang, M.J. (2003), Tandem PDZ repeats in glutamate receptor-interacting proteins have a novel mode of PDZ domain-mediated target binding, *Nat. Struct. Biol.* **10**, 972-978.

Fields, G.B. and Noble, R.L. (1990), Solid-Phase Peptide-Synthesis Utilizing 9-Fluorenylmethoxycarbonyl Amino-Acids, *Int. J. Pept. Protein Res.* **35**, 161-214.

Fogh, R., Ionides, J., Ulrich, E., Boucher, W., Vranken, W., Linge, J.P., Rieping, W., Bhat, T.N., Westbrook, J., Henrick, K., Gilliland, G., Berman, H., Thornton, J., Nilges, M., Markley, J., and Laue, E. (2002), The CCPN project: an interim report on a data model for the NMR community, *Nat. Struct. Biol.* **9**, 416-418.

Garrett, D.S., Seok, Y.J., Peterkofsky, A., Clore, G.M., and Gronenborn, A.M. (1997), Identification by NMR of the binding surface for the histidine-containing phosphocarrier protein HPr on the N-terminal domain of enzyme I of the Escherichia coli phosphotransferase system, *Biochemistry (Mosc).* **36**, 4393-4398.

Glerum, D.M., Shtanko, A., and Tzagoloff, A. (1996), Characterization of COX17, a yeast gene involved in copper metabolism and assembly of cytochrome oxidase, *J. Biol. Chem.* **271**, 14504-14509.

Goto, J.J., Zhu, H.N., Sanchez, R.J., Nersissian, A., Gralla, E.B., Valentine, J.S., and Cabelli, D.E. (2000), Loss of in vitro metal ion binding specificity in mutant copper-zinc superoxide dismutases associated with familial amyotrophic lateral sclerosis, *J. Biol. Chem.* **275**, 1007-1014.

Grootjans, J.J., Reekmans, G., Ceulemans, H., and David, G. (2000), Syntenin-syndecan binding requires syndecan-synteny and the co-operation of both PDZ domains of syntenin, *J. Biol. Chem.* **275**, 19933-19941.

Guntert, P., Mumenthaler, C., and Wuthrich, K. (1997), Torsion angle dynamics for NMR structure calculation with the new program DYANA, *J. Mol. Biol.* **273**, 283-298.

Harris, B.Z., Hillier, B.J., and Lim, W.A. (2001), Energetic determinants of internal motif recognition by PDZ domains, *Biochemistry (Mosc).* **40**, 5921-5930.

Harrison, M.D., Jones, C.E., and Dameron, C.T. (1999), Copper chaperones: function, structure and copper-binding properties, *Journal of Biological Inorganic Chemistry* **4**, 145-153.

Heaton, D.N., George, G.N., Garrison, G., and Winge, D.R. (2001), The mitochondrial copper metallochaperone Cox17 exists as an oligomeric, polycopper complex, *Biochemistry (Mosc).* **40**, 743-751.

Helgstrand, M., Kraulis, P., Allard, P., and Hard, T. (2000), Ansig for Windows: An interactive computer program for semiautomatic assignment of protein NMR spectra, *J. Biomol. NMR* **18**, 329-336.

Herrmann, T., Guntert, P., and Wuthrich, K. (2002), Protein NMR structure determination with automated NOE assignment using the new software CANDID and the torsion angle dynamics algorithm DYANA, *J. Mol. Biol.* **319**, 209-227.

Hillier, B.J., Christopherson, K.S., Prehoda, K.E., Bredt, D.S., and Lim, W.A. (1999), Unexpected modes of PDZ domain scaffolding revealed by structure of nNOS-syntrophin complex, *Science* **284**, 812-815.

Himelblau, E., Mira, H., Lin, S.J., Culotta, V.C., Penarrubia, L., and Amasino, R.M. (1998), Identification of a functional homolog of the yeast copper homeostasis gene ATX1 from Arabidopsis, *Plant Physiol.* **117**, 1227-1234.

Hiromura, M., Chino, H., Sonoda, T., and Sakurai, H. (2000), Molecular cloning and characterization of a copper chaperone for copper/zinc superoxide dismutase from the rat, *Biochem. Biophys. Res. Commun.* **275**, 394-400.

Hiromura, M. and Sakurai, H. (1999), Molecular cloning of rat ATX1 homologue protein, *Biochem. Biophys. Res. Commun.* **265**, 509-512.

Ho, C.S., Marinescu, V., Steinhilb, M.L., Gaut, J.R., Turner, R.S., and Stuenkel, E.L. (2002), Synergistic effects of Munc18a and X11 proteins on amyloid precursor protein metabolism, *J. Biol. Chem.* **277**, 27021-27028.

Im, Y.J., Lee, J.H., Park, S.H., Park, S.J., Rho, S.H., Kang, G.B., Kim, E., and Eom, S.H. (2003), Crystal structure of the Shank PDZ-ligand complex reveals a class IPDZ interaction and a novel PDZ-PDZ dimerization, *J. Biol. Chem.* **278**, 48099-48104.

Jelen, F., Oleksy, A., Smietana, K., and Otlewski, J. (2003), PDZ domains - common players in the cell signaling, *Acta Biochim. Pol.* **50**, 985-1017.

Jensen, L.T., Posewitz, M.C., Srinivasan, C., and Winge, D.R. (1998), Mapping of the DNA binding domain of the copper-responsive transcription factor Mac1 from Saccharomyces cerevisiae, *J. Biol. Chem.* **273**, 23805-23811.

Joshi, A., Serpe, M., and Kosman, D.J. (1999), Evidence for (Mac1p)(2)center dot DNA ternary complex formation in Mac1p-dependent transactivation at the CTR1 promoter, *J. Biol. Chem.* **274**, 218-226.

Kaminskaia, N.V. and Kostic, N.M. (1998), Alcoholysis of urea catalyzed by palladium(II) complexes, *Inorganic Chemistry* **37**, 4302-4312.

Kang, B.S., Cooper, D.R., Devedjiev, Y., Derewenda, U., and Derewenda, Z.S. (2003a), Molecular roots of degenerate specificity in syntenin's PDZ2 domain: Reassessment of the PDZ recognition paradigm, *Structure* **11**, 845-853.

Kang, B.S., Cooper, D.R., Jelen, F., Devedjiev, Y., Derewenda, U., Dauter, Z., Otlewski, J., and Derewenda, Z.S. (2003b), PDZ tandem of human syntenin: Crystal structure and functional properties, *Structure* **11**, 459-468.

Kannt, A., Young, S., and Bendall, D.S. (1996), The role of acidic residues of plastocyanin in its interaction with cytochrome f, *Biochim. Biophys. Acta* **1277**, 115-126.

Keller, R. (2004), The Computer Aided Resonance Assignment Tutorial,

Klomp, L.W.J., Lin, S.J., Yuan, D.S., Klausner, R.D., Culotta, V.C., and Gitlin, J.D. (1997), Identification and functional expression of HAH1, a novel human gene involved in copper homeostasis, *J. Biol. Chem.* **272**, 9221-9226.

Knight, S.A.B., Labbe, S., Kwon, L.F., Kosman, D.J., and Thiele, D.J. (1996), A widespread transposable element masks expression of a yeast copper transport gene, *Genes & Development* **10**, 1917-1929.

Koradi, R., Billeter, M., and Wuthrich, K. (1996), MOLMOL: A program for display and analysis of macromolecular structures, *J. Mol. Graph.* **14**, 51-&.

Labbe, S., Zhu, Z.W., and Thiele, D.J. (1997), Copper-specific transcriptional repression of yeast genes encoding critical components in the copper transport pathway, *J. Biol. Chem.* **272**, 15951-15958.

Lamb, A.L., Torres, A.S., O'Halloran, T.V., and Rosenzweig, A.C. (2001), Heterodimeric structure of superoxide dismutase in complex with its metallochaperone, *Nat. Struct. Biol.* **8**, 751-755.

Lamb, A.L., Wernimont, A.K., Pufahl, R.A., Culotta, V.C., O'Halloran, T.V., and Rosenzweig, A.C. (1999), Crystal structure of the copper chaperone for superoxide dismutase, *Nat. Struct. Biol.* **6**, 724-729.

Laskowski, R.A., Macarthur, M.W., Moss, D.S., and Thornton, J.M. (1993), Procheck - a Program to Check the Stereochemical Quality of Protein Structures, *Journal of Applied Crystallography* **26**, 283-291.

Lee, D.S., Tomita, S., Kirino, Y., and Suzuki, T. (2000), Regulation of X11L-dependent amyloid precursor protein metabolism by XB51, a novel X11L-binding protein, *J. Biol. Chem.* **275**, 23134-23138.

Lim, K., Ho, J.X., Keeling, K., Gilliland, G.L., Ji, X.H., Ruker, F., and Carter, D.C. (1994), 3-Dimensional Structure of Schistosoma-Japonicum Glutathione-S-Transferase Fused with A 6-Amino Acid Conserved Neutralizing Epitope of Gp41 from Hiv, *Protein Sci.* **3**, 2233-2244.

Lin, S.J., Pufahl, R.A., Dancis, A., Ohalloran, T.V., and Culotta, V.C. (1997), A role for the Saccharomyces cerevisiae ATX1 gene in copper trafficking and iron transport, *J. Biol. Chem.* **272**, 9215-9220.

Linge, J.P., Williams, M.A., Spronk, C., Bonvin, A., and Nilges, M. (2003), Refinement of protein structures in explicit solvent, *Proteins-Structure Function and Genetics* **50**, 496-506.

Lipari, G. and Szabo, A. (1982a), Model-Free Approach to the Interpretation of Nuclear Magnetic-Resonance Relaxation in Macromolecules .1. Theory and Range of Validity, *J. Am. Chem. Soc.* **104**, 4546-4559.

Lipari, G. and Szabo, A. (1982b), Model-Free Approach to the Interpretation of Nuclear Magnetic-Resonance Relaxation in Macromolecules .2. Analysis of Experimental Results, *J. Am. Chem. Soc.* **104**, 4559-4570.

Lockhart, P.J. and Mercer, J.F.B. (2000), Identification of the copper chaperone SAH in Ovis aries: expression analysis and in vitro interaction of SAH with ATP7B, *Biochimica Et Biophysica Acta-Gene Structure and Expression* **1490**, 11-20.

Long, J.F., Tochio, H., Wang, P., Fan, J.S., Sala, C., Niethammer, M., Sheng, M., and Zhang, M.J. (2003), Supramodular structure and synergistic target binding of the N-terminal tandem PDZ domains of PSD-95, *J. Mol. Biol.* **327**, 203-214.

Mandel, A.M., Akke, M., and Palmer, A.G. (1995), Backbone Dynamics of Escherichia-Coli Ribonuclease Hi - Correlations with Structure and Function in an Active Enzyme, *J. Mol. Biol.* **246**, 144-163.

Martins, L.J., Jensen, L.T., Simons, J.R., Keller, G.L., and Winge, D.R. (1998), Metalloregulation of FRE1 and FRE2 homologs in Saccharomyces cerevisiae, *J. Biol. Chem.* **273**, 23716-23721.

Maximov, A., Sudhof, T.C., and Bezprozvanny, I. (1999), Association of neuronal calcium channels with modular adaptor proteins, *J. Biol. Chem.* **274**, 24453-24456.

McLoughlin, D.M., Standen, C.L., Lau, K.F., Ackerley, S., Bartnikas, T.P., Gitlin, J.D., and Miller, C.C.J. (2001), The neuronal adaptor protein X11 alpha interacts with the copper chaperone for SOD1 and regulates SOD1 activity, *J. Biol. Chem.* **276**, 9303-9307.

Milovic, N.M. and Kostic, N.M. (2001), Palladium(II) and Platinum(II) complexes as synthetic peptidases, *Probing of Proteins by Metal Ions and Their Low-Molecular-Weight Complexes* **38**, 145-186.

Milovic, N.M. and Kostic, N.M. (2002), Palladium(II) complexes, as synthetic peptidases, regioselectively cleave the second peptide bond "upstream" from methionine and histidine side chains, *J. Am. Chem. Soc.* **124**, 4759-4769.

Milovic, N.M. and Kostic, N.M. (2003), Palladium(II) complex as a sequence-specific peptidase: Hydrolytic cleavage under mild conditions of X-Pro peptide bonds in X-Pro-Met and X-Pro-His segments, *J. Am. Chem. Soc.* **125**, 781-788.

Nabuurs, S.B., Nederveen, A.J., Vranken, W., Doreleijers, J.F., Bonvin, A., Vuister, G.W., Vriend, G., and Spronk, C. (2004), DRESS: a database of REfined solution NMR structures, *Proteins-Structure Function and Bioinformatics* **55**, 483-486.

Nabuurs, S.B., Spronk, C., Krieger, E., Maassen, H., Vriend, G., and Vuister, G.W. (2003), Quantitative evaluation of experimental NMR restraints, *J. Am. Chem. Soc.* **125**, 12026-12034.

Nishihara, E., Furuyama, T., Yamashita, S., and Mori, N. (1998), Expression of copper trafficking genes in the mouse brain, *Neuroreport* **9**, 3259-3263.

O'Halloran, T.V. and Culotta, V.C. (2000), Metallochaperones, an intracellular shuttle service for metal ions, *J. Biol. Chem.* **275**, 25057-25060.

Okamoto, M. and Sudhof, T.C. (1997), Mints, Munc18-interacting proteins in synaptic vesicle exocytosis, *J. Biol. Chem.* **272**, 31459-31464.

Okamoto, M. and Sudhof, T.C. (1998), Mint 3: A ubiquitous mint isoform that does not bind to munc18- 1 or -2, *Eur. J. Cell Biol.* **77**, 161-165.

Palmer, A., Zimmer, M., Erdmann, K.S., Eulenburg, V., Porthin, A., Heumann, R., Deutsch, U., and Klein, R. (2002), EphrinB phosphorylation and reverse signaling: regulation by Src kinases and PTP-BL phosphatase, *Mol. Cell* **9**, 725-737.

Pena, M.M.O., Lee, J., and Thiele, D.J. (1999), A delicate balance: Homeostatic control of copper uptake and distribution, *J. Nutr.* **129**, 1251-1260.

Pena, M.M.O., Puig, S., and Thiele, D.J. (2000), Characterization of the Saccharomyces cerevisiae high affinity copper transporter Ctr3, *J. Biol. Chem.* **275**, 33244-33251.

Pufahl, R.A., Singer, C.P., Peariso, K.L., Lin, S.J., Schmidt, P.J., Fahrni, C.J., Culotta, V.C., PennerHahn, J.E., and Ohalloran, T.V. (1997), Metal ion chaperone function of the soluble Cu(I) receptor Atx1, *Science* **278**, 853-856.

Qiao, F., Hu, J.Z., Zhu, H.Z., Luo, X.M., Zhu, L.G., and Zhu, D.X. (1999), Site-specific hydrolysis of horse heart cytochrome c and apocytochrome c promoted by palladium(II) complex, *Polyhedron* **18**, 1629-1633.

Rae, T.D., Schmidt, P.J., Pufahl, R.A., Culotta, V.C., and O'Halloran, T.V. (1999), Undetectable intracellular free copper: The requirement of a copper chaperone for superoxide dismutase, *Science* **284**, 805-808.

Rosenzweig, A.C., Huffman, D.L., Hou, M.Y., Wernimont, A.K., Pufahl, R.A., and O'Halloran, T.V. (1999), Crystal structure of the Atx1 metallochaperone protein at 1.02 angstrom resolution, *Structure* **7**, 605-617.

Rosenzweig, A.C. and O'Halloran, T.V. (2000), Structure and chemistry of the copper chaperone proteins, *Curr. Opin. Chem. Biol.* **4**, 140-147.

Schmidt, P.J., Kunst, C., and Culotta, V.C. (2000), Copper activation of superoxide dismutase 1 (SOD1) in vivo - Role for protein-protein interactions with the copper chaperone for SOD1, *J. Biol. Chem.* **275**, 33771-33776.

Schmidt, P.J., Rae, T.D., Pufahl, R.A., Hamma, T., Strain, J., O'Halloran, T.V., and Culotta, V.C. (1999), Multiple protein domains contribute to the action of the copper chaperone for superoxide dismutase, *J. Biol. Chem.* **274**, 23719-23725.

Schwieters, C.D., Kuszewski, J.J., Tjandra, N., and Clore, G.M. (2003), The Xplor-NIH NMR molecular structure determination package, *J. Magn. Reson.* **160**, 65-73.

Senn, H., Werner, B., Messerle, B.A., Weber, C., Traber, R., and Wuthrich, K. (1989), Stereospecific Assignment of the Methyl H-1-Nmr Lines of Valine and Leucine in Polypeptides by Nonrandom C-13 Labeling, *FEBS Lett.* **249**, 113-118.

Silahtaroglu, A.N., Jensen, L.R., Harboe, T.L., Horn, P., Bendixen, C., Tommerup, N., and Tumer, Z. (2004), Sequencing and mapping of the porcine CCS gene, *Anim. Genet.* **35**, 353-354.

Solioz, M., Portmann, R., and Stoyanov, J. (2003), Copper homeostasis in E-hirae, *J. Inorg. Biochem.* **96**, 54.

Srinivasan, C., Posewitz, M.C., George, G.N., and Winge, D.R. (1998), Characterization of the copper chaperone Cox17 of Saccharomyces cerevisiae, *Biochemistry (Mosc).* **37**, 7572-7577.

Tomita, S., Fujita, T., Kirino, Y., and Suzuki, T. (2000), PDZ domain-dependent suppression of NF-kappa B/p65-induced A beta 42 production by a neuron-specific X11-like protein, *J. Biol. Chem.* **275**, 13056-13060.

Ubbink, M. and Bendall, D.S. (1997), Complex of plastocyanin and cytochrome c characterized by NMR chemical shift analysis, *Biochemistry (Mosc).* **36**, 6326-6335.

Vaccaro, P. and Dente, L. (2002), PDZ domains: troubles in classification, *FEBS Lett.* **512**, 345-346.

van den Berk, L.C., van Ham, M.A., te Lindert, M.M., Walma, T., Aelen, J., Vuister, G.W., and Hendriks, W.J. (2004), The interaction of PTP-BL PDZ domains with RIL: an enigmatic role for the RIL LIM domain., *Mol. Biol. Rep.* **31**, 203-215.

van Ham, M. and Hendriks, W. (2003), PDZ domains - glue and guide, *Mol. Biol. Rep.* **30**, 69-82.

Vriend, G. (1990), What If - a Molecular Modeling and Drug Design Program, *J. Mol. Graph.* **8**, 52-56.

Waggoner, D.J., Bartnikas, T.B., and Gitlin, J.D. (1999), The role of copper in neurodegenerative disease, *Neurobiol. Dis.* **6**, 221-230.

Wakabayashi, T., Nakamura, N., Sambongi, Y., Wada, Y., Oka, T., and Futai, M. (1998), Identification of the copper chaperone, CUC-1, in Caenorhabditis elegans: Tissue specific co-expression with the copper transporting ATPase, CUA-1, *FEBS Lett.* **440**, 141-146.

Walma, T. (2004), **Thesis**: The second PDZ domain of PTP-BL, Radboud Universiteit Nijmegen, *Chapter 6 p. 109-140*.

Walma, T., Spronk, C.A.E.M., Tessari, M., Aelen, J., Schepens, J., Hendriks, W., and Vuister, G.W. (2002), Structure, dynamics and binding characteristics of the second PDZ domain of PTP-BL, *J. Mol. Biol.* **316**, 1101-1110.

Wishart, D.S. and Sykes, B.D. (1994), Chemical-Shifts as a Tool for Structure Determination, *Nuclear Magnetic Resonance, Pt C* **239**, 363-392.

Wong, P.C., Waggoner, D., Subramaniam, J.R., Tessarollo, L., Bartnikas, T.B., Culotta, V.C., Price, D.L., Rothstein, J., and Gitlin, J.D. (2000), Copper chaperone for superoxide dismutase is essential to activate mammalian Cu/Zn superoxide dismutase, *Proc. Natl. Acad. Sci. U. S. A.* **97**, 2886-2891.

Worrall, J.A.R., Kolczak, U., Canters, G.W., and Ubbink, M. (2001), Interaction of yeast iso-1-cytochrome c with cytochrome c peroxidase investigated by [N-15,H-1] heteronuclear NMR spectroscopy, *Biochemistry (Mosc).* **40**, 7069-7076.

Worrall, J.A.R., Liu, Y.J., Crowley, P.B., Nocek, J.M., Hoffman, B.M., and Ubbink, M. (2002), Myoglobin and cytochrome b(5): A nuclear magnetic resonance study of a highly dynamic protein complex, *Biochemistry (Mosc).* **41**, 11721-11730.

YamaguchiIwai, Y., Serpe, M., Haile, D., Yang, W.M., Kosman, D.J., Klausner, R.D., and Dancis, A. (1997), Homeostatic regulation of copper uptake in yeast via direct binding of MAC1 protein to upstream regulatory sequences of FRE1 and CTR1, *J. Biol. Chem.* **272**, 17711-17718.

Zhu, L., Bakhtiar, R., and Kostic, N.M. (1998), Transition-metal complexes as alternatives to proteolytic enzymes. Regioselective cleavage of myoglobin by palladium(II) aqua complexes, *Journal of Biological Inorganic Chemistry* **3**, 383-391.

Zimmermann, P., Meerschaert, K., Reekmans, G., Leenaerts, I., Small, J.V., Vandekerckhove, J., David, G., and Gettemans, J. (2002), PIP2-PDZ domain binding controls the association of syntenin with the plasma membrane, *Mol. Cell* **9**, 1215-1225.

Samenvatting

Eiwitten zijn belangrijke macromoleculen van de levende wereld. Gedurende het ontstaan, de groei en uiteindelijk de dood van de levende cel, zorgen eiwitten voor de overdracht van signalen binnenin de cel en tussen cellen onderling. Eiwitten maken ongeveer 15% van de massa van de cel uit, en hun wisselwerking speelt een rol in elk celproces, zoals in de synthese en afbraak van DNA/RNA, in de synthese, vouwing en afbraak van eiwitten, in de signaaloverdracht, in de regulering van de activiteit van eiwitten, en in het immuunsysteem.

Een goed begrip van de wisselwerking tussen eiwitten is daarom essentieel voor het begrijpen van alle processen die zich afspelen in de cel, en uiteindelijk ook voor het ontwikkelen van manieren om verstoorde processen te herstellen.

In de loop van hun synthese verkrijgen bepaalde eiwitten een cofactor, bijvoorbeeld een metaalion. Metalen zijn essentiele componenten van eiwitten die betrokken zijn in metabole processen zoals de ademhaling of fotosynthese. Maar deze metalen kunnen ook giftig zijn voor cellen en daarom bezitten de cellen van elk organisme een systeem dat de metalen verwerkt. Deze systemen zijn specifiek voor elk type metaal en meer of minder complex al naar gelang het organisme.

Een voorbeeld hiervan is te vinden in bakkersgist. Het transportsysteem van koper in dit organisme omvat een membraaneiwit dat het metaal toegang verleend tot het inwendige van de cel (zie Figuur 1.1**A**). Vervolgens wordt het metaal door een zogenaamd chaperone-eiwit, CCS, getransporteerd naar zijn eindbestemming, in dit geval het eiwit SOD1. Het C-terminale domein van CCS, genaamd CCSIII, speelt een belangrijke rol in het overbrengen van het koperion van CCS naar SOD1.

Onlangs is ontdekt dat CCS ook een wisselwerking kan vertonen met een neuronaal eiwit (X11α) met als gevolg dat de werking van SOD1 verstoord wordt. Het blijkt dat SOD1 inactief wordt als het PDZ2-domein van X11α (PDZ2α in het vervolg) een wisselwerking vertoont met CCSIII.

Het onderzoek zoals gepresenteerd in dit proefschrift heeft als doel het karakteriseren van de interactie tussen CCSIII en PDZ2α.

Eerst is de structuur (i.e. de driedimensionale vorm) in oplossing bepaald van PDZ2α met behulp van kernspinresonantie (Nuclear Magnetic Resonance, NMR). Eerst zijn de ^{1}H, ^{13}C en ^{15}N NMR spectra toegekend (**Hoofdstuk 2**) en vervolgens zijn deze resonantiegegevens gebruikt voor het bepalen van de structuur van het PDZ2α domein (**Hoofdstuk 3**). Het ensemble van de 20 beste modellen uit de berekening laat een eenduidig gevormde structuur zien, die alle voor PDZ domeinen gebruikelijke elementen bevat, te weten zes β-sheets en twee α-helices. Opmerkelijk is dat de uit de resonanties voorspelde structuur duidt op kleinere secundaire structuurelementen en op slechts vier β-sheets. De superpositie van de beste van deze modellen met de structuur van twee andere PDZ domeinen (Psd-95-PDZ3 en PTP-BL-PDZ2) toont twee bijzondere kenmerken van PDZ2α (Figuur 3.2**B**): de loop L1 is langer dan in andere PDZ domeinen, terwijl de loop L2 korter blijkt. De bindingsite van het ligand daarentegen, is, zoals verwacht, gelocaliseerd tussen de sheet βB en de helix αB. Het is voorts interessant om te zien dat de tussen de PDZ-domeinen geconserveerde aminozuren, i.e. Gln 25 tot Phe 28, zich bevinden in een positie die gunstig is voor interactie met de liganden, ondanks de grotere lengte van loop L1.

Ten tweede is de interactie tussen PDZ2α en CCSIII gedetaileerd in kaart gebracht (**Hoofdstuk 4**). Hiertoe is gebruik gemaakt van de gevoeligheid van de chemische verschuiving voor de omgeving van de betrokken kern. Wanneer de ligand gebonden wordt, verandert de chemische omgeving van kernen dicht bij de bindingsplaats, wat leidt tot veranderingen in de NMR spectra. Spectra van PDZ2α in de afwezigheid en aanwezigheid van verscheidene synthetische peptiden afgeleid van CCSIII zijn onderling vergeleken teneinde te bepalen welke aminozuren van CCSIII wisselwerking vertonen met welke aminozuren van PDZ2α. Het onderzoek van twee peptiden zoals afgeleid van CCSIII toont aan dat PDZ2α C-terminale aminozuren van CCS bindt (Ac-AQPPAHL), met een dissociatieconstante ter

grootte van 91 ± 2 μM, en dat PDZ2α en Ac-AQPPAHL een snelle uitwisseling vertonen, in de orde van 1000 s⁻¹.

Om het relatieve belang van elk residu vast te stellen zijn vijf varianten van Ac-AQPPAHL bestudeerd: Ac-AQPPAHL**-NH₂**, waarin de C-terminale carboxygroep geneutraliseerd is, **A**QPPAHL, waarin de N-terminus van het peptide niet geneutraliseerd is (dus positief geladen) en Ac-AQPPAH**A**, Ac-AQPPA**A**L en Ac-AQP**A**AHL, waarin de betrokken residuen vervangen zijn door een alanine. De resultaten van dit onderzoek staan vermeld in Tabel 4.1 en zijn weergegeven in Figuur 4.6.

Allereerst blijkt uit deze resultaten dat de beschikbaarheid van de C-terminale carboxygroep een absolute voorwaarde is voor de interactie tussen PZ2α en de peptide van CCSIII, omdat Ac-AQPPAHL-NH₂ in het geheel niet bindt aan PDZ2α. Dit laatste komt waarschijnlijk doordat elektrostatische interactie tussen de carboxy-terminal groep en de zijgroep van Arg 19 niet meer mogelijk is.

Verder is aangetoond dat de belangrijkste residuen van de peptide in de verbinding de leucine en de histidine zijn. De residuen van PDZ2α die het meest beinvloed worden door het peptide met de leucinevariant (Ac-AQPPAH**A**) zijn de hydrofobe residuen van de bindingsholte. Echter, slechts één residu van PDZ2α (Gly 27 van het geconserveerde bindingsmotief) lijkt beinvloed te worden door de histidinevariant van het peptide (Ac-AQPPA**A**L). Het is opmerkelijk dat histidine niet het gunstigste residu is, omdat Ac-AQPPA**A**L beter bindt aan PDZ2α dan Ac-AQPPAHL. Dit zou verklaard kunnen worden uit een wellicht aanwezige waterstof binding tussen de histidinezijgroep en de C-terminale carboxygroep van het peptide.

Overigens blijkt de aanwezigheid van een positieve lading op de N-terminus van het peptide slechts een klein effect te hebben op de affiniteit van PDZ2α voor CCSIII, en de substitutie van het C-terminaal proline residu helemaal geen effect.

Tenslotte is een verkennende studie uitgevoerd naar de mogelijkheid van het gebruik van palladiumbevattende moleculen als zeer specifieke proteasen (**Hoofdstuk 5**). Deze moleculen, ontwikkeld door Professor N. Kostic van Iowa State University USA, vertonen proteaseactiviteit, maar uitsluitend onder pH- en

temperatuursomstandigheden die de eiwitten doen denatureren. Echter, het mechanisme van de reactie suggereert dat de mogelijkheid bestaat om te werken onder mildere omstandigheden indien het palladium bindt aan een Pro-Met sequentie in het te klieven eiwit.

Het doel van het onderzoek was het testen van de proteolytische activiteit van twee palladiumbevattende moleculen, cis-[Pd(en)(H_2O)$_2$](ClO$_4$)$_2$ en [Pd(H_2O)$_4$](ClO$_4$)$_2$, op een chimaer-eiwit dat samengesteld is uit PDZ2α, een Pro-Met sequentie en een tag (His$_6$-GST), teneinde de tag en het PDZ2α domein te scheiden na zuivering. Onder de toegepaste experimentele omstandigheden is het niet mogelijk gebleken de effectiviteit van de palladiumderivaten aan te tonen. Hiervoor zijn verscheidene mogelijke verklaringen. Het chimaer-eiwit bevat 7% aan aminozuurresiduen die in staat zijn om het palladium te binden. Wellicht dient het experiment herhaald te worden met een groter overmaat aan palladiumderivaten, of met een andere tag.

Dit onderzoek is het eerste in een serie van studies met als doel het ontwikkelen van een nieuwe generatie proteasen die het scheiden van het onderzochte eiwit en zijn tag mogelijk maakt onder niet-denaturerende omstandigheden.

Résumé

Parmi les macromolécules nécessaires à tout organisme vivant, on trouve les acides nucléiques, les polysaccharides (sucres complexes) et les protéines. Ces dernières représentent environ 15 % de la masse cellulaire. Tout au long de la vie des cellules, ces macromolécules interagissent entre elles et permettent le bon fonctionnement de la cellule. Ainsi les interactions protéine-protéine sont impliquées dans toutes les étapes de la vie cellulaire telles que : la synthèse, la dégradation des acides nucléiques (ADN/ARN), la synthèse, le repliement et la dégradation des protéines, la transmission de signaux (à l'intérieur de la cellule et également entre cellules), la régulation de l'activité des protéines, et la réponse immunitaire. Ces interactions sont finement régulées et une perturbation de ces interactions peut être à l'origine de situations pathologiques.

Comprendre ces interactions est donc d'une importance primordiale si l'on veut comprendre les événements cellulaires, et développer à terme des traitements permettant de corriger les situations pathologiques.

Au cours de leur maturation, certaines protéines acquièrent un cofacteur, tel qu'un métal, indispensable à leur activité. Ces métaux bien qu'essentiels pour de nombreux processus biologiques vitaux (respiration, photosynthèse) peuvent s'avérer toxiques s'ils ne sont pas pris en charge correctement. C'est pourquoi les cellules de chaque organisme disposent d'un système de transport des métaux. Ces systèmes sont spécifiques à chaque métal, et plus ou moins complexes selon l'organisme.

Ainsi chez la levure (*Saccharomyces cerevisiae*), le système de transport du cuivre comporte une protéine membranaire chargée de faire passer le métal à l'intérieur de la cellule (voir Figure 1.1**A**). Celui-ci est ensuite pris en charge par une protéine dite chaperonne (ici, la CCS), qui l'amène jusqu'à sa destination finale, c'est-à-dire la protéine cible nécessitant ce métal (en l'occurrence la SOD1). Cette protéine chaperonne (CCS) possède un domaine particulier, le domaine III, dont le rôle est prépondérant dans ce mécanisme. Récemment, il a été découvert que la CCS

pouvait également interagir avec une autre protéine, la protéine neuronale (X11α) avec comme conséquence l'inactivation de SOD1. Cette inactivation résulte de l'interaction entre le domaine PDZ2 de la protéine X11α (PDZ2α dans la suite du texte) et le domaine CCSIII (voir Figure 1.1**B**).

Les travaux de recherche, présentés dans ce manuscrit, décrivent les résultats que nous avons obtenus lors de la caractérisation des interactions entre les domaines CCSIII et PDZ2α.

Dans un premier temps, nous avons déterminé la structure (*i.e.* la forme tridimensionnelle) du domaine PDZ2α, en solution, par spectroscopie par résonance magnétique nucléaire (RMN). Tout d'abord nous avons attribué les déplacements chimiques des atomes (H, C et N) du domaine PDZ2α (**Chapitre II**), qui ont par la suite permis de calculer une structure pour le domaine PDZ2α (**Chapitre III**). L'ensemble des 20 meilleurs modèles issus du calcul montre que le domaine PDZ2α possède une structure bien définie, comportant tous les éléments caractéristiques des domaines PDZ. Ainsi PDZ2α est constitué de six feuillets β et de deux hélices α. Il est intéressant de noter que la structure prédite uniquement à partir des déplacements chimique indiquait des éléments de structure secondaire de plus petite taille et seulement quatre feuillets β. La comparaison du meilleur de ces modèles avec la structure de deux autres domaine PDZ connus (Psd-95-PDZ3 et PTP-BL-PDZ2) montre que la structure de PDZ2α est singulière en deux points. En effet celui-ci possède une boucle L1 plus longue et *a contrario* une boucle L2 plus courte. Cependant, il est intéressant de noter que le site de liaison des ligands demeure bien formé, entre le feuillet βB et l'hélice αB. De même, les résidus acides aminés conservés entre domaines PDZ, *i.e.* Gln 25 à Phe 28, sont maintenus dans une orientation favorable pour interagir avec le(s) ligand(s).

La suite de notre étude a consisté à caractériser les interactions entre PDZ2α et CCSIII (**Chapitre IV**). Pour cela, nous avons également utilisé la RMN, et la propriété des déplacements chimiques des atomes à varier avec un changement d'environnement. Le principe est que les déplacements chimiques des atomes de

PDZ2α seront différents selon qu'ils sont ou non en contact avec un ligand. PDZ2α a donc été observé en absence et en présence de plusieurs peptides synthétiques dérivés de CCSIII. Les spectres RMN ainsi obtenus ont été comparés afin de déterminer quels sont les résidus de CCSIII et de PDZ2α qui interagissent. L'étude de deux peptides dérivés de CCSIII a montré que PDZ2α lie les résidus situé en position C-terminale de CCS (Ac-AQPPAHL où Ac- indique que le groupe amino-terminal est protégé par un groupe acétyl) avec une constante de dissociation de l'ordre de 91 ± 2 μM, et que les deux partenaires sont en échange rapide avec un k_{off} de l'ordre de 1000 s^{-1}.

Pour établir l'importance relative de chaque résidu, cinq variants de peptide Ac-AQPPAHL ont été étudiés : Ac-AQPPAHL**-NH2** où le groupe carboxy-terminal est neutralisé, **A**QPPAHL où le groupe N-terminal est déprotégé, Ac-AQPPAH**A**, Ac-AQPPA**A**L, et Ac-AQP**A**AHL où les résidus soulignés et en caractères gras ont été substitués pour une alanine. Les résultats de notre étude (résumés dans le Tableau 4.1 et sur la Figure 4.6) montrent que la présence du groupe carboxy-terminal libre est absolument nécessaire à l'interaction entre PDZ2α et le peptide de CCS puisque Ac-AQPPAHL**-NH2** est incapable de se lier à PDZ2α. Ceci est probablement lié au fait que l'interaction électrostatique entre le groupe carboxy-terminal avec la chaîne latérale de Arg 19 *via* une molécule d'eau ne peut plus se faire.

L'étude des autres peptides a montré que les résidus les plus importants dans la liaison sont, par ordre croissant, la leucine puis l'histidine. Les résidus de PDZ2α les plus touchés par le variant de la leucine (Ac-AQPPAH**A**) sont les résidus hydrophobes formant la poche de liaison. En revanche, un seul résidu de PDZ2α (Gly 27 du motif de liaison conservé) semble affecté par le variant de l'histidine (Ac-AQPPA**A**L).

Il est intéressant de noter que l'histidine n'est pas le résidu le plus favorable dans la mesure où PDZ2α présente une affinité plus forte pour Ac-AQPPA**A**L que pour le peptide originel. Ceci peut être expliqué par une possible liaison hydrogène entre la chaîne latérale de l'histidine et le groupe carboxy-terminal du peptide, déplaçant ainsi légèrement l'équilibre (voir Figure 4.6).

Enfin, l'absence de protection du groupe N-terminal n'a qu'un effet modéré, et la substitution de la proline C-terminale n'a aucun effet sur l'affinité de PDZ2α pour le peptide de CCS.

Pour finir, une étude préliminaire sur la possibilité d'utiliser des composés dérivés du palladium entant que protéases de haute spécificité a été menée (**Chapitre V**). Ces composés ont été développés dans le laboratoire du Professeur N. Kostic (université de l'état d'Iowa, USA). Ces composés ont prouvé leur efficacité, mais dans des conditions de pH et de température dénaturantes pour les protéines. Cependant, le mécanisme de clivage par ces composés suggère que ceux-ci pourraient être efficaces dans des conditions douces pour les protéines à condition que ces composés soient ancrés sur un motif Pro–Met de la protéine à cliver.

Cette étude représente donc la première d'une série d'expériences visant au développement d'une génération de nouvelles protéases permettant de séparer une protéine d'intérêt de son ancre peptidique, dans des conditions non dénaturantes, ceci afin de restaurer la protéine native.

Au cours de notre étude nous avons pu tester la capacité protéolytique de deux composés à base de palladiums, le (cis-$[Pd(en)(H_2O)_2](ClO_4)_2$ et $[Pd(H_2O)_4](ClO_4)_2$) sur une protéine chimère constituée du domaine PDZ2α, d'une séquence linker Pro–Met, et d'une ancre (His_6–GST). L'objectif est le clivage sélectif de l'ancre peptidique (Tag) du domaine PDZ2α après purification. Les conditions testées ici n'ont pas permis de démontrer l'efficacité de ces composés à base de palladium. Plusieurs raisons sont imputables à cela. Tout d'abord, la protéine chimère contient 7 % de résidus capables de lier le palladium. Il faudrait donc répéter ces essais avec un excès plus large de palladium, ou avec l'utilisation d'un autre tag. D'autre part, le milieu tampon peut être un facteur d'échec, et devra donc être optimisé au cours des études ultérieures.

Cette étude est la première d'une série d'expériences visant au développement d'une génération nouvelle de protéases afin de séparer une protéine d'intérêt de son tag, dans des conditions non dénaturantes, permettant l'étude de la protéine en question.

List of abbreviations

CcP: cytochrome *c* peroxidase

CCS: copper chaperone for SOD1

CSI: chemical shift index

cyt *c*:   cytochrome *c*

E.coli: *Escherichia coli*

en: ethylenediamine

Fmoc: 9-fluorenylmethoxycarbonyl

GST: glutathione S-tranferase

HOAc: acetic acid

Mb: myoglobin

NMM: N-methylmorpholine

NMP: N-methylpyrrolidone

NMR: nuclear magnetic resonance

Pc: plastocyanin

PCR: polymerase chain reaction

Pd: palladium

PDZ: post-synaptic density-95 protein, *Drosophila* disks-large protein A, *zona occludens* protein 1

PyBOP: benzotriazole-1-yl-oxy-tris-pyrrolidino-phosphonium hexafluoro-phosphate

RP-HPLC: reversed phase high-performance liquid chromatography

SOD1:   superoxide dismutase 1

TFA: trifluoroacetic acid

Acknowledgments

Here we are, at the end of the journey that is a PhD. It's been sometimes a lot of fun, and sometimes long and difficult. Therefore it's been an amazingly enriching experience. And I have been fortunate enough to meet a lot of nice people who have helped in one way or another, who have been supportive and whom I would like to thank dearly.

I will start with my family. They might not be aware of how, but without them I would not have been where I am now. *Omain, 'Pa* : sans vous, il est évident que je n'en serais jamais arrivée où j'en suis, à bien des égards. Je vous suis reconnaissante de tout ce que vous m'avez donné l'occasion de connaître et d'accomplir ; je voudrais profiter de ces quelques lignes pour vous dire de ne pas oublier à quel point vous comptez autant l'un que l'autre pour moi. *Ma (g……☺) Taine*, évidemment un grand merci pour ton aide dans la préparation de ma soutenance ; bon, maintenant que tout ça est fini, j'espère rentrer bientôt, pas trop loin de toi. Je vous aime tous fort.

I also would like to address a few words to the people who have introduced me to Science and research. Cher *Alain*, tu n'es évidemment pas étranger à mon parcours. Je te remercie de m'avoir accueillie dans ton labo et de m'avoir fait découvrir la recherche si jeune. *Hervé, Nan*, merci de votre patience et de votre temps.

Joséfina, Virgine de P7: il semble écrit que mes amis les plus proches seront aussi les plus éloignés en distance ! Ma foi, ainsi soit-il! Merci d'être mes amies, mais ne vous éloignez pas trop quand même ☺.

Then I arrived in "the country of the low sky", where I've met an amazing amount of people, so diverse in their cultures and qualities. I'm sorry I'll only name a few here. *Alan, Chico*, I am thankful for your company and friendship; I will never forget the wonderful time we had at Plantage 16, our uncontrollable laughters (often just before Sam entered the kitchen somehow!) and the priceless moments spent together. I wish you weren't so far away physically. *Sharm*, "the girl next door" ☺: thank you for your warm heart and mind, and thank you for introducing me to your world (women magazines and real Asian food! "onder anderen"); it was great to know you were just "a wall away", literally or metaphorically. *Manu*: I am grateful to you for your artistic touch to this book. You have a great mind and great talents so… "Chill out, babe!" ☺. *Gerhild, Virginie*: thank you for making the last few months so fun, it's a pity that we've met only recently.

Marcellus: I owe you so much that I cannot even express my gratitude in the right terms; I enjoyed very much interacting with you, whether it was on a professional level or during our French meetings.

During my PhD time, I had the privilege to be working at the Radboud Universiteit in Nijmegen with *Chris, Sander, Hugo* and *Marlies*: I would like to thank you all dearly for your warmth and knowledge sharing and patience with me; *Geerten*, I simply cannot thank you enough!

After a productive day spent at the RUN, I could stay at the Verhoeven Family House. Lieve *Annemiek, Ad* and *Carlijn*: ik wil van harte jullie bedanken voor jullie gezelligheid, steun en vriendschap. Ik vond het heerlijk om bij jullie te zijn.

I also would like to thank dearly my paranimfs *Rob* and *Taine*: thank you for seating next to me, supporting me during the ceremony and just making this day a lot easier.

Michiel: you've been there everyday for a large part of my PhD. To you, I just want to say this: tout seul c'est bien, à deux c'est mieux.

Finally, to all my friends: as I wrote in French above, my closest friends seem to end up being the farthest in distance for some reason. Well, c'est la vie! Thank you all for being my friends, but please don't go too far!

Curriculum Vitae

Aude Duquesne was born on the 22nd of May 1977 in Coulommiers, France. She meets science and research at the age of 16, in the group of Prof. L. Sedel. After graduating from the local high school, Lycee Jules Ferry, at the age of 17, she moves to Paris to study biology at University Paris 7. There, she became aware of her attraction for contacts with people from international origins. During her 4th year, she went to Leiden for a six months training within the Erasmus exchange programme in Prof. Dr. G.W. Canters, under the supervision of Dr. M. Ubbink and worked on the "development of a covalent paramagnetic probe for NMR studies". Then she went back to Paris for one year to finish her degree and spend one year in the lab of Prof. Dr. J. Josefonwicz, purifying and characterizing the α-L-fucosidase from scallops. After her graduation in 1999, she had the opportunity to go back to Leiden, for her PhD in the Metallo-Protein group of Prof. Dr. G.W. Canters. There, she has studied the interaction Parts of this thesis were presented orally during the Dutch annual Protein Research Meeting (Studiegroep Eiwitonderzoek, Lunteren, The Netherlands, 2004).